Journal of Environmental Management 348 (2023) 119240

Contents lists available at ScienceDirect

Journal of Environmental Management

journal homepage: www.elsevier.com/locate/jenvman

Research article

Distinct diversity patterns and assembly mechanisms of prokaryotic microbial sub-community in the water column of deep-sea cold seeps

Yuanjiao Lyu [a,1], Jian Zhang [a,1], Yu Chen [b], Qiqi Li [a], Zhixin Ke [a], Si Zhang [a,b], Jie Li [a,*]

[a] CAS Key Laboratory of Tropical Marine Bio-resources and Ecology, South China Sea Institute of Oceanology, Chinese Academy of Sciences, Guangzhou, 510301, China
[b] Southern Marine Science and Engineering Guangdong Laboratory (Guangzhou), Guangzhou 511458, China

ARTICLE INFO

Handling Editor: Prof Raf Dewil

ABSTRACT

Methane leakage from deep-sea cold seeps has a major impact on marine ecosystems. Microbes sequester methane in the water column of cold seeps and can be divided into abundant and rare groups. Both abundant and rare groups play an important role in cold seep ecosystems, and the environmental heterogeneity in cold seeps may enhance conversion between taxa with different abundances. Yet, the environmental stratification and assembly mechanisms of these microbial sub-communities remain unclear. We investigated the diversities and assembly mechanisms in microbial sub-communities with distinct abundance in the deep-sea cold seep water column, from 400 m to 1400 m. We found that bacterial β-diversity, as measured by Sørensen dissimilarities, exhibited a significant species turnover pattern that was influenced by several environmental factors including depth, temperature, SiO_3^{2-}, and salinity. In contrast, archaeal β-diversity showed a relatively high percentage of nestedness pattern, which was driven by the levels of soluble reactive phosphate and SiO_3^{2-}. During the abundance dependency test, abundant taxa of both bacteria and archaea showed a significant species turnover, while the rare taxa possessed a higher percentage of nestedness. Stochastic processes were prominent in shaping the prokaryotic community, but deterministic processes were more pronounced for the abundant taxa than rare ones. Furthermore, the metagenomics results revealed that the abundances of methane oxidation, sulfur oxidation, and nitrogen fixation-related genes and related microbial groups were significantly higher in the bottom water. Our results implied that the carbon, sulfur, and nitrogen cycles were potentially strongly coupled in the bottom water. Overall, the results obtained in this study highlight taxonomic and abundance-dependent microbial community diversity patterns and assembly mechanisms in the water column of cold seeps, which will help understand the impacts of fluid seepage from the sea floor on the microbial community in the water column and further provide guidance for the management of cold seep ecosystem under future environmental pressures.

1. Introduction

Deep-sea cold seeps are unique seafloor chemosynthetic ecosystems fueled by the release of deeply sourced hydrocarbon-rich fluids. These deep sources of matter and energy, primarily methane and other hydrocarbons, support diverse benthic fauna and microbes and impact marine biogeochemical cycles (Cruaud et al., 2015; Ke et al., 2022; Orcutt et al., 2011; Ruff et al., 2015). While fluids released from cold seeps create an undersea oasis, releasing greenhouse gases, including methane, into the air significantly affects the climate (Feng et al., 2018; Wang et al., 2017b; Wei et al., 2020). Previous studies have shown that the organisms in sediments and the sediment-seawater interface consume ~20–80% of the methane emitted by cold seeps (Boetius and Wenzhofer, 2013), suggesting there is still a large amount of methane diffusion into the overlaying water. Methane oxidation in the upper water column of cold seeps has been documented, suggesting that microbes are an important barrier to intercepting methane in the water column of cold seeps (Cao et al., 2021; Hansman et al., 2017; Savvichev et al., 2018). In addition, in the dark ocean (>200 m) above the cold seep, microorganisms serve as an important primary production, and the energy captured by them enters into other nodes of the ecosystem through predation or symbiosis (Mattes et al., 2013; Orcutt et al., 2011). Given the fundamental role of microorganisms in driving the biogeochemical cycles and primary production in the overlying water column

* Corresponding author.
E-mail address: lijietaren@scsio.ac.cn (J. Li).
[1] These authors contributed equally to this paper and should be considered as co-first author.

https://doi.org/10.1016/j.jenvman.2023.119240
Received 29 May 2023; Received in revised form 5 September 2023; Accepted 2 October 2023
Available online 12 October 2023

of cold seep, it is essential to understand the distribution characteristics, assembly mechanisms, and environmental drivers of these microbial communities.

The physicochemical factors are known to vary with the depth gradient of the ocean, such as temperature, salinity, and dissolved oxygen, which affects the microbial communities exhibiting depth stratification (Frank et al., 2016; Lindh et al., 2017; Qian et al., 2011; Sunagawa et al., 2015). Beyond the cold seep, the deep hydrocarbon fluids discharged into the water column create diversified and heterogeneous habitats in time and space, which leads to more complex factors shaping microbial communities (Feng et al., 2022; Pop Ristova et al., 2012; Ruff et al., 2015). There is an increasing consensus that the availability of methane and oxygen in the water column has a significant impact on the aerobic methane oxidation process (Boetius and Wenzhofer, 2013; Li et al., 2022). Another study emphasized the importance of environmental heterogeneity to microbial taxa assembly in the water column around cold seeps (Huang et al., 2023). In summary, depth (Zhang et al., 2020c), temperature (Huang et al., 2023), gradients of electron acceptors and donors (Schreiber et al., 2010; Vigneron et al., 2014), and biological interactions (Cruaud et al., 2015) can affect microbial community composition in the cold methane seeps environment. It has been shown that bacterial community compositions significantly diverged with a variation of seepage intensity in the bottom water of cold seeps, but the archaeal community exhibited similarities among different sites (Zhang et al., 2020c). Therefore, it has been suggested that environmental factors may have differential impacts on archaea and bacteria in the cold seep water column.

A cognitive understanding of the ecological processes and mechanisms that determine the assembly of microbial communities is central to maintaining the function of ecosystems in the global oceans (Milke et al., 2022; Song et al., 2022; Sunagawa et al., 2015). Within the quantitative ecological framework, the ecological processes of microbial β-diversity have been identified as dispersal limitation and environmental selection, and it is necessary to clarify the underlying variations of microbial diversity spatially (Dini-Andreote et al., 2015; Landeiro et al., 2018; Zhang et al., 2020b). Baselga proposed a method of calculating the partitioning of β-diversity in 2010 (Baselga, 2010). This method involves using Sørensen dissimilarity matrices to break down β-diversity into two components: species turnover and nestedness. Species turnover refers to variations in community diversity resulting from the replacement of species (Specziár et al., 2018), while nestedness refers to disparities in species richness that occur when one community is a subset of a more diverse community (Legendre, 2014). With this approach, several studies have discussed changes in diversity and potential distribution mechanisms of microbiomes in a variety of habitats (lakes, reservoirs, and oceans) along gradient factors, such as sediment stratification, water depth, and nitrogen enrichment (Rasmussen et al., 2021; Wu et al., 2020; Xue et al., 2018; Zhang et al., 2021). Accumulating evidence suggests that microbial communities exhibit divergent distribution patterns along the marine environmental gradients (Li et al., 2021a; Liu et al., 2018; Tobias-Hunefeldt et al., 2019), but how the partitioning of microbial β-diversity (species turnover and nestedness) varies with water depth, together with its response characteristics to the local factors in the water column above cold seeps remain unknown.

With significant inroads achieved in sequencing technology over the past few years, many studies have begun to focus on the microbial biogeography and assembly mechanisms of rare taxa in marine ecosystems (Hugoni et al., 2013; Sogin et al., 2006; Wu et al., 2017). The rare taxa were defined as a potential seed bank with high genetic and functional diversity (Lennon and Jones, 2011), and several studies examining the interactions of microbial taxa have indicated that rare taxa occupied critical nodes for maintaining network links and stability (Xue et al., 2018; Zhang et al., 2020a; Zhang et al., 2022). The process of transitioning from rarity to abundance has been widely reported in several microbial groups, such as those found in rivers and oceans, and has been linked to changes in environmental factors such as depth, temperature, and seasonal variations (Campbell et al., 2011; Hugoni et al., 2013; Zhang et al., 2022). The environmental heterogeneity of cold seeps may enhance conversion between taxa with different abundances. Different assemblage mechanisms are anticipated to affect abundant and rare community structures (Lindh et al., 2017; Xue et al., 2018). For instance, previous study showed that abundant taxa are mostly impacted by dispersal limitations, whereas rare taxa are primarily influenced by environmental filtering in the northwestern Pacific Ocean (Wu et al., 2017). Understanding the assemblage mechanisms of abundant and rare microbial communities that drive the formation of ecological communities is essential for effective ecosystem management (Liu et al., 2019). However, the partitioning of β-diversity patterns and assemblages mechanisms of abundant and rare prokaryotic microorganisms, particularly in the water column above cold seeps, have not been investigated.

The Haima cold seep area is approximately 350 km^2 and is primarily formed by temporally transported methane leakage in the South China Sea. Continuous methane fluid leaks from top sediments into the underlying water column in this area (Feng et al., 2018; Liang et al., 2017). Thus, the Haima cold seep is ideal for examining the dual action of environmental gradient and seep plume on the microbial community assembly at a regional scale. To investigate the microbial diversity, functions, and underlying assembly mechanisms in the water column of cold seeps, especially in the dark ocean, we sampled a set of depth gradients (400–1400 m) located in the Haima cold seeps. In this study, we elucidated the β-diversity components and assembly mechanisms of bacterial and archaeal sub-communities and explored the function distribution in the dark ocean at a seep plume regional scale.

2. Materials and methods

2.1. Study region and sampling

The Haima cold seeps are located on the lower continental slope of the northwestern SCS (South China Sea) at a depth of roughly 1360–1400 m and cover an area of about 618 km^2, of which about 350 km^2 have been explored for active cold seeps, and are primarily made up of time-space migrated methane leaks. Five stations (HM1-HM5) situated within the Haima cold seeps (Fig. 1a) were selected for the collection of seawater samples in September 2020. At each station, microbial samples were systematically collected from the water column at depths of 400, 600, 750, 1000, 1200, 1300, and 1400 m using Conductivity-Temperature-Depth equipment (CTD) outfitted with Niskin sample bottles. Samples of bottom water (collected at 1400 m) were obtained through the use of a remotely operated vehicle ("Haima" ROV). In-situ measurements of dissolved oxygen (DO), salinity, and temperature were carried out using Sea-Bird 911 CTD (Sea-Bird Electronics, Washington, USA). Water samples were filtered using 0.22 μm pore size filters (Whatman, Clifton, NJ, USA) and kept at −80 °C for microbiological analysis. Laboratory experiments were performed using a flow injection autoanalyzer (Lacht QC 8500) to measure a wide variety of seawater environmental factors., including ammonium (NH_4^+), nitrite (NO_2^-), nitrate (NO_3^-), dissolved inorganic nitrogen (DIN), silicate (SiO_3^{2-}), and soluble reactive phosphorus (SRP).

2.2. DNA extraction, full-length 16 S rRNA gene amplification, sequencing, and analysis

TGuide S96 Magnetic Beads Genomic DNA Extraction Kit for Nucleic Acid Extraction was used to extract microbial DNA from cold seep samples according to the manufacturer's guidelines. The whole 16 S rRNA gene was amplified using a 30 μL PCR reaction volume. The primers for bacterial and archaeal amplification are 27 F/1492 R pairs and A1F/1490 R pairs (Lam et al., 2020). The PCR thermal cycle began at 95 °C for 2 min, followed by 25 cycles at 98 °C for 10 s, 55 °C for 30 s, 72 °C for 90 s, and a final extension at 72 °C for 2 min. The amplification

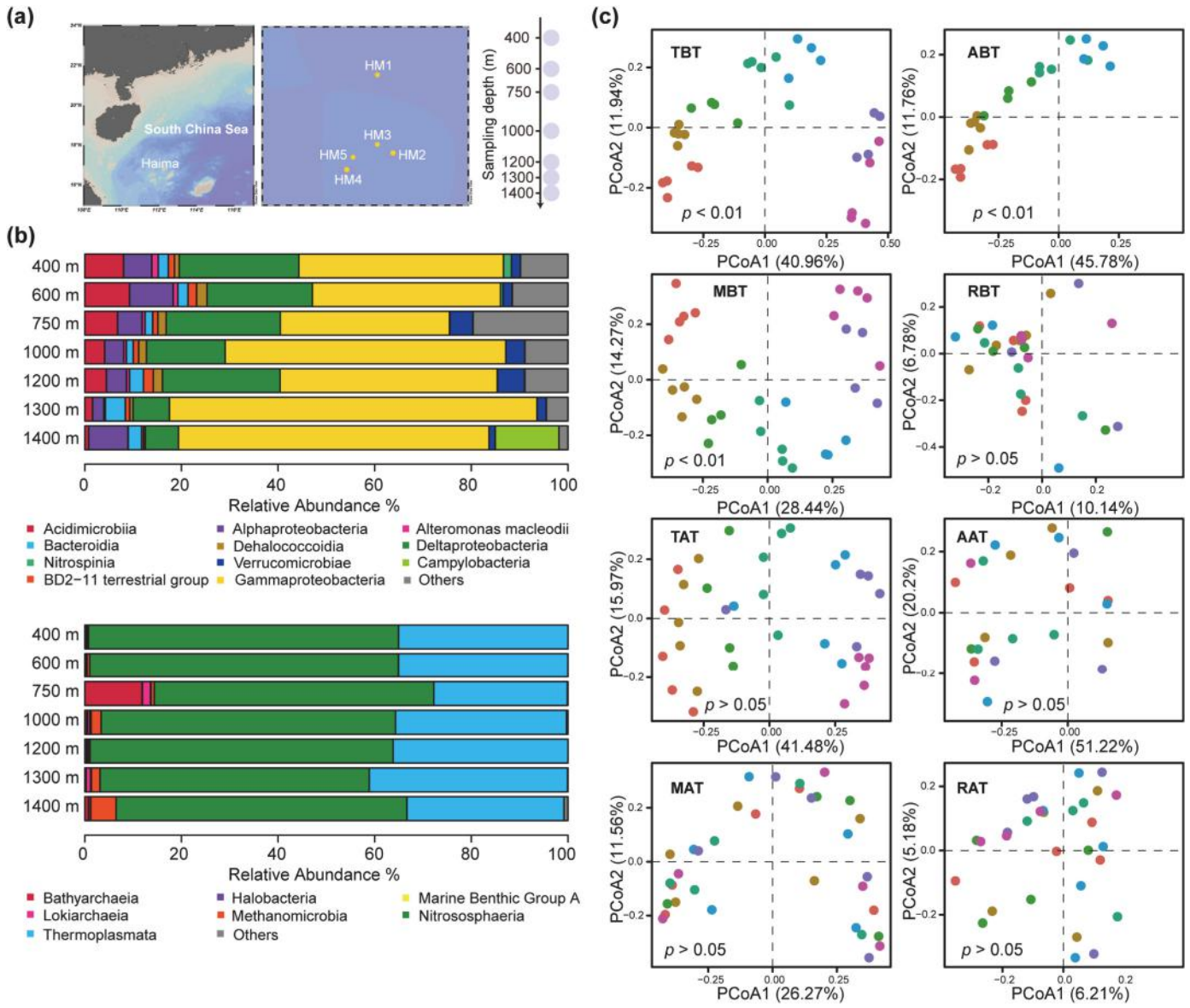

Fig. 1. (a) The sampling sites (HM1-HM5) at the South China Sea, Haima cold seeps; (b) the relative abundance of bacterial and archaeal communities at the class level in the water column above cold seeps; (c) Principal coordinate analysis (PCoA) plots for bacterial and archaeal sub-communities based on the Bray–Curtis dissimilarity matrix, the *p*-value indicates the significance of the results from the ANOSIM test based on grouping at different depths. Abbreviations: total bacterial taxa (TBT), abundant bacterial taxa (ABT), moderate bacterial taxa (MBT), rare bacterial taxa (RBT), total archaeal taxa (TAT), abundant archaeal taxa (AAT), moderate archaeal taxa, and rare archaeal taxa (RAT).

products were examined for concentration (Qubit), and bands (agarose gel electrophoresis), and the qualifying samples were mixed. The mixed product was prepared for library construction using PacBio's SMRTbell Template Prep Kit. The reaction products were purified with AMpure PB Beads (Pacbio, USA) and sequenced on a Pacbio Sequel II sequencer. The raw data were corrected to obtain Circular Consensus Sequencing (CCS) reads (SMRT Link, version 8.0). With minPasses ≥6 and minpasses ≥0.9. Lima (v1.7.0) software was subsequently used to eliminate the chimeras to produce high-quality CCS sequences. CCS sequences not containing primers were discarded and filtered according to CCS length. Sequences that did not meet the length threshold (16 S: 1200bp-1650bp) were discarded using Cutadapt (v2.7). Amplicon sequence variants (ASVs) were produced in QIIME2 (v2020.6) (Bolyen et al., 2019) using DADA2 (Callahan et al., 2016), which filters ASVs by 0.005% of the total number of sequences sequenced as a threshold. SILVA database (Quast et al., 2012) (release 132) was used for the taxonomic annotation of the feature sequences, and a simple Bayesian classifier combined with a comparison approach was used to retrieve the taxonomic information of the species corresponding to each feature. The amplicon sequencing data used in this study are all available in the NCBI Sequence Read Archive (SRA) under the accession number PRJNA953740.

All ASVs were classified into four classes (Xue et al., 2018), including abundant taxa (AT): average relative abundance ≥0.01% in each water layer or ≥ 1% in at least one water layer; moderate taxa (MT): average relative abundance scoping from 0.01% to 1% in each water layer; rare taxa (RT): average relative abundance <0.01% in at least one water layer, but never ≥1% in any water layer.

To quantify habitat specialization, the "niche breadth index (NBI)" approach was used for sub-communities (Levins, 1968). ASVs with a greater NBI were present and distributed more uniformly on a large scale. A lower NBI, on the other hand, indicated that ASVs were found in fewer habitats and were distributed unevenly (Pandit et al., 2009). We estimated the NBI for each sub-community based on species abundance and evenness, and this analysis was conducted using the 'niche width'

function in the 'spaa' package.

To investigate the β-diversity of three sub-communities in the water column above cold seeps, we used Baselga's approach to calculate β-diversity components. Based on the Sørensen dissimilarity index, total diversity (β_{total}) was divided into species turnover (β_{turn}) and nestedness (β_{nest}) difference components using the R package adespatial (Baselga, 2010; Shen et al., 2020).

2.3. Metagenomic sequencing and analysis

To further characterize seawater microbiome functions, we used 35 DNA samples from the water column above cold seeps for metagenomic sequencing using the Illumina sequencing platform. Raw reads were filtered using fastp software to obtain high-quality sequencing data. MEGAHIT (Version 1.1.2) (Dinghua et al., 2015) was used to assemble the macrogenome, filtering contigs less than 300 bp. The assembly results were evaluated using the QUAST software (Gurevich et al., 2013). Using the default parameters, the MetaGeneMark software (Version 3.26) was used to identify the coding areas in the genome (Hyatt et al., 2012). MMseqs2 (Version 11-e1a1c) was used to reduce redundancy, using a similarity criterion of 95% and a coverage level of 90% (Steinegger and Söding, 2017). Functional annotation was carried out by comparing the protein sequences of non-redundant genes to those in the Kyoto Encyclopedia of Genes and Genomes (KEGG) database. Based on the cycling pathways observed across all metagenomic samples, the genes related to methane, nitrogen, and sulfur cycles were selected and filtered out. The metagenome sequencing data were submitted to the NCBI Sequence Read Archive (SRA) under the accession number PRJNA954901.

2.4. Statistical analyses

A one-way ANOVA was conducted to explore changes in alpha diversity indices, taxon relative abundance, and relative abundance of functional genes along a depth gradient, followed by Tukey's post hoc tests (utilizing a 0.05 threshold of significance). The Kruskal-Wallis ANOVA was utilized for non-parametric data. Principal coordinate analysis (PCoA) based on Bray-Curtis distances was used to examine changes in the microbial community structure. To assess whether these shifts differed significantly across depths, an analysis of similarities (ANOSIM) was performed. To investigate the associations between microbial community structure and local factors, we conducted a redundancy analysis (db-RDA). Further, the significant ($p < 0.05$) local factors were selected for variation partitioning analysis (VPA). VPA was performed to determine the relative contributions of the measured temperature, nutrient (NH_4^+, NO_3^-, NO_2^-, SRP, SiO_3^{2-}), and dissolved oxygen. Mantle tests and partial Mantle tests (999 permutations) were used to investigate the connections between the local factors and β-diversity components (species turnover and nestedness). The above analyses were carried out using the vegan package in R (v4.1.3).

2.5. Co-occurrence network construction

Co-occurrence networks were generated to examine the interactions within the microbial community composition (using bacterial and archaeal ASVs) and function (using nitrogen, sulfur, and methane metabolism genes) in the water column above cold seeps with the psych package in R. The networks were constructed using pairwise Spearman's rank correlations from more than 50% of the samples. Interactions with a coefficient of correlation >0.7 and p-value <0.05 after Benjamin Hochberg adjustment were included in networks. Network statistics such as average path, degree, and average clustering coefficient were determined to clarify the network's patterns. A module is a collection of nodes more strongly linked to one another than nodes outside the module. The value of modularity (M), which has a threshold of M values > 0.4, indicates how well a network is separated into modules (Newman, 2006). The network hub analysis was based on each node's connectivity, which was determined by within-module and among-module connectivity (Zi and Pi) (Deng et al., 2012). Furthermore, 1000 Erdös-Réyni random networks with the same number of nodes and edges as the genuine networks were built, with each edge having the same possibility of being assigned to any node. Topology features such as modularity, average clustering coefficient, and average path were determined and compared for real and random networks. Gephi (version 0.9.2) was used for network visualization.

2.6. Neutral community model (NCM)

A neutral community model (NCM) was used to quantify the influence of deterministic and stochastic processes on the assembly of microbial communities (Sloan et al., 2006). The "Hmisc" and "minpack.lm" packages in R software were used to construct the NCM. The R^2 values measure the goodness of fit to the NCM, and higher R^2 values imply that neutral processes are more significant than environmental selection in community assembly, as predicted by the neutral model. We calculated 95% confidence intervals for all fitting statistics using bootstrapping with 1000 repeats (Chen et al., 2019; Sloan et al., 2006). Furthermore, we explored the impact of stochastic processes on microbial species with varying abundances in the model.

3. Results

3.1. Environmental parameters along the water depth gradient

The vertical profiles of the environmental factors are exhibited in Fig. S1. We observed significant differences in environmental properties along the depth gradient, including a sharp decrease in temperature from 400 m (10.3 °C) to 1400 m (2.9 °C). Dissolved oxygen (DO) concentrations gradually decreased and reached a nadir at 750 m, though they subsequently showed a certain degree of increase. Salinity was observed to increase along the water depth. Besides, the vertical profiles for ammonium nitrogen (NH_4^+), nitrate nitrogen (NO_3^-), nitrite nitrogen (NO_2^-), soluble reactive phosphorus (SRP), and silicate (SiO_3^{2-}) exhibited an increasing trend.

3.2. The microbial community composition along the water depth gradient

All bacterial amplicon sequence variants (ASVs) were classified as abundant bacterial taxa (ABT) (22.44%), moderate bacterial taxa (MBT) (30.61%), and rare bacterial taxa (RBT) (30.61%). All archaeal ASVs were categorized as abundant archaeal taxa (AAT) (2.69%), moderate archaeal taxa (Mattes et al.) (15.06%), and rare archaeal taxa (RAT) (82.24%). The most dominant bacterial phylum was Proteobacteria, which accounted for 63.71%–85.96% along the depth gradient, followed by Marinimicrobia SAR406 clade (1.49%–10.58%), Actinobacteria (0.83%–9.37%), and Bacteroidetes (1.42%–2.88%) (Fig. 1b). Alphaproteobacteria, Deltaproteobacteria, and Gammaproteobacteria were the dominant classes of Proteobacteria that were observed. Deltaproteobacteria (6.85%–24.78) showed a significant downward trend, with the lowest proportion at the bottom (Fig. 1b). However, Gammaproteobacteria (34.98%–64.29%) exhibited an opposite trend as it reflected an upward trend. The dominant archaeal phyla included Thaumarchaeota (57.10%–64.53%) and Euryarchaeota (31.06%–40.74%) (Fig. 1b). The archaeal fractions at all depths were principally populated by the Thaumarchaeota (57.10%–64.53%) and Euryarchaeota (31.06%–40.74%). The Nitrososphaeria clade was among the most abundant across the entire depth gradient, with relative abundances between 56.94% and 63.72%. Thermoplasmata also exhibited a wide distribution along the water columns, accounting for 30.05%–37.62%. The third most abundant class overall was Methanomicrobia (range 0.72%–3.77%).

The distribution pattern of functional taxa related to the

biogeochemical cycles was analyzed with respect to depth (Fig. S2). The profile characteristics revealed that groups of functional taxa differed in their distribution pattern, thereby indicating niche partitioning. The LS-NOB (Nitrospinaceae), which was represented by ASV_294 (MBT) and ASV_416 (MBT), was observed at a depth ranging from 400 m to 1200 m and gradually decreased in abundance. Contrary to these findings, Nitrincolaceae (ASV_152), which belonged to ABT, was only present at a depth of 1200–1400 m. Moreover, Nitrosopumilaceae had higher relative abundance in the different water layers, accounting for 43.38%–56.92%. The bacterial communities of hydrocarbon metabolism were also assessed for their depth distribution characteristics in the water column of cold seeps. For example, the Methylomonaceae, Methylophilaceae, and Cycloclasticaceae distribution exhibited gradually increasing distribution along the water column. At 1300 m and 1400 m, a higher abundance of the Methylotrophic Group 2 (Methylomonaceae) and Milano-WF1B-03 (Methylomonaceae), which were represented by ASV_24 (ABT), ASV_276 (ABT), ASV_293 (ABT), ASV_86 (ABT), and ASV_73 (ABT), was observed. *Methylotenera* (Methylophilaceae), which consisted of ASV_111 (ABT) and ASV_375 (MBT), was mainly distributed in the deeper water layers, especially around 1300 m and 1400 m, with a relative abundance of up to 83.73%. Similarly, *Cycloclasticus* (Cycloclasticaceae, ASV_424, which belongs to MBT) was only present from 1200 m to 1400 m. However, no obvious gradient distribution pattern with depth was observed for anaerobic methane-oxidizing archaea. These archaea consisted of ANME-1a, ANME-1b, ANME-2c, ANME-2a-2b, and ANME-3, represented by 1 ASV of AAT, 10 ASV of MAT, and 64 ASV of RAT. The microbial taxa involved in the sulfur cycle also showed different distribution patterns. *Sulfurovum* showed a narrow distribution predominantly enriched in the bottom layer (13.16%). The relative abundances of two ASVs associated with the *Sulfurovum* (ASV_194 and ASV_64, which belong to ABT) were 1.73% and 6.01% at 1400 m, respectively. The SUP05 cluster (Thioglobaceae) exhibited a decreasing distribution trend along the water columns, with higher abundances only observed at the 400 m and 600 m depths (10.23% and 11.21%, respectively), as represented by ASV_131 (ABT), ASV_215 (ABT), ASV_34 (ABT), ASV_262 (MBT), ASV_345 (MBT), and ASV_355 (MBT). On the other hand, ASV_177 (MBT) and ASV_207 (ABT) were mainly distributed in deeper water layers. Moreover, SEEP-SRB1, SEEP-SRB2, and SEEP-SRB4, which consisted of RBT, were dispersed in different water layers.

3.3. The microbial community diversity and driving factors

The analyzed alpha diversities of bacterial and archaeal communities included the Shannon, Phylogenetic diversity (PD), and Chao1 indices (Table S1). When comparing each layer sample, there was no obvious divergence along the depth gradient ($P > 0.05$). Meanwhile, principal coordinate analysis was performed to investigate segregation patterns between bacterial and archaeal taxa in the water column. (Fig. 1c). We observed that the samples from different layers were clearly separated during principal coordinate analysis. The first principal coordinate explained 40.96%, 28.44%, 41.48%, and 26.27% of the variation for the TBT, ABT, MBT, and RBT, respectively. Similarly, for the TAT, AAT, MAT, and RAT, the first principal coordinate explained 45.78%, 10.14%, 51.22%, and 6.21% of the variation, respectively. The ANOSIM results showed that the bacterial community structures (TBT, ABT, MBT) varied significantly with depth, while the structure of the RBT was similar (Table S2). The archaeal communities (TAT, MAT, TAT, and RAT) exhibited no significant gradient distribution structure along the gradient depth (Table S2).

Mantel tests and partial Mantel tests corroborated microbial community dissimilarity was correlated with environmental parameters in the water column (Fig. S3a). Overall, the results showed that TBT, ABT, MBT, RBT, and TAT were associated with local factors ($p < 0.05$). Moreover, partial Mantel tests revealed that bacterial community (TBT, ABT, MBT, and RBT) strongly correlated with depth and NH_4^+. We also observed that the depth, NH_4^+, and SiO_3^{2-} were associated with the TAT, but the three archaeal sub-communities (AAT, MAT, and RAT) did not significantly correlate with environmental parameters in the water column above cold seeps. Furthermore, db-RDA was performed to evaluate the correlations between environmental factors and microbial community structures (Fig. S3b). The db-RDA results revealed that two axes (db-RDA1 and db-RDA2) could explain 10%–40% of the bacterial sub-taxa variance, while the db-RDA1 and db-RDA2 accounted for 7%–33% of the archaeal sub-taxa variance. SiO_3^{2-}, DO, NH_4^+, and temperature were significantly correlated with the three bacterial sub-taxa structures. Interestingly, only SiO_3^{2-}, DO, and temperature correlated with the total archaeal sub-taxa structures ($p < 0.05$). Furthermore, canonical VPA (Fig. S3c) was used to determine the percentage of variation explained by nutrients (NH_4^+, NO_3^-, NO_2^-, SRP, SiO_3^{2-}), temperature, O_2 their combined effect on both bacterial and archaeal communities (Fig. S3c). The temperature and nutrients were the groups of factors that significantly explained most of the variability for TBT (temperature: 39%, nutrients: 36%), ABT (temperature: 43%, nutrients: 40%) and TAT (temperature: 34%, nutrients: 32%). The explanatory power of temperature, nutrients, and oxygen is relatively low for rare taxa (RBT: 4%, RAT: 0.37%).

3.4. The partitioning of microbial β-diversity varies with local factors

To explore the variations in components of β-diversity, Baselga's approach was used to conduct β-diversity decomposition analyses (Fig. 2a). We found that the TBT contribution of species turnover (β_{turn}) was higher than nestedness (β_{nest}) ($P < 0.001$) (79.520% vs. 20.480%, respectively) (Fig. S4a, Table 1). For ABT, MBT, and RBT, the β-diversity (β_{Total}) was dominated by the β_{turn} (contributed 74.495%, 77.590%, and 56.609%), while β_{nest} only contributed 25.505%, 22.410%, and 43.391%, respectively (β_{turn} significantly higher than β_{nest}, $P < 0.001$) (Fig. S4a, Table 1). Comparison of sub-community diversity showed β_{nest} and β_{nest} of RBT was significantly higher than other sub-communities ($P < 0.001$). The β_{Total} of TAT, AAT, and MAT was primarily attributed to β_{turn} (51.532%, 54.809%, and 56.057%, respectively), while β_{nest} of RAT was significantly greater than β_{turn} (Fig. S4b, Table 1). Meanwhile, the β_{nest} of RAT was significantly greater than other sub-communities ($P < 0.001$). Further analysis of the horizontal β_{Total} within the samples from the same water depth (Fig. S5) revealed that the β_{turn} dominated the β_{Total} of bacterial communities, while the β_{nest} had a higher proportion for archaeal communities.

The partial Mantel tests showed that the β_{Total} and β_{turn} of bacterial communities strongly correlated with depth, temperature, SiO_3^{2-}, and salinity (Fig. 2b). NH_4^+ also exhibited a significant effect on the β_{nest} of TBT, ABT, and MBT, as well as the β_{turn} of RBT. SRP, SiO_3^{2-}, and DO were the three main environmental variables influencing archaeal β-diversity components (Fig. 2b). Furthermore, the depth-decay regression analysis was conducted to demonstrate the influence of depth on β-diversity and its components (β_{turn} and β_{nest}) (Fig. S6). There were significant and positive relationships between the depth distance and β_{Total} and β_{turn} of bacterial communities, while archaeal sub-communities β-diversity (β_{Total}, β_{turn}, and β_{nest}) exhibited no obvious correlation with depth distance.

3.5. The potential mechanisms for microbial community assembly

To explore mechanisms responsible for community assembly underlying the observed gradient patterns, deterministic and stochastic processes were analyzed with the neutral community model (Fig. 3a). The NCM explained 68.3% and 52.6% of the bacterial and archaeal communities, respectively, suggesting that deterministic processes (gradient variance of local factors) have a paramount influence on bacterial and archaeal community assembly. Moreover, in the neutral model, the points that significantly deviated from the neutral community model suggested that the taxa may be influenced by the surrounding

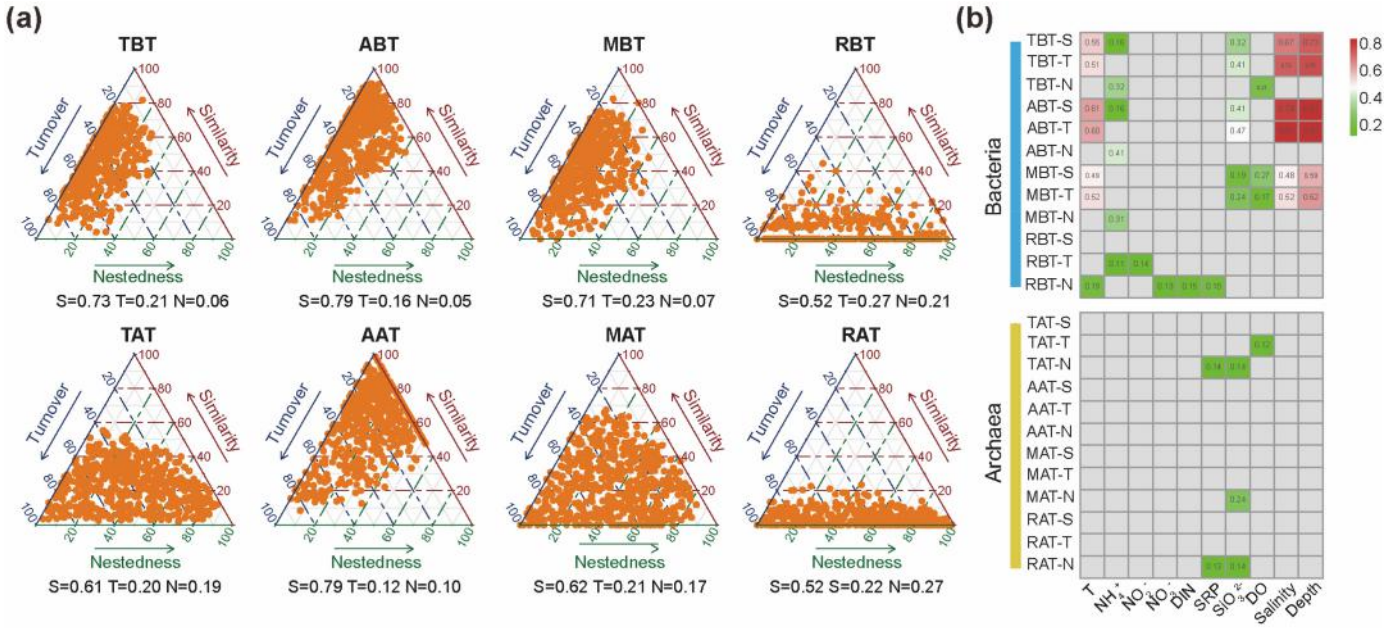

Fig. 2. (a) Triangular plots of β-diversity components for bacterial and archaeal communities based on the Sørensen dissimilarities matrix in all water layers. Three different values from the S (similarity), T (species turnover), and N (nestedness) matrices determine the location of each point; (b) partial Mantel tests for the relationship between microbial community β-diversity components (species turnover and nestedness) and local factors, the gray fill indicates no significant correlation and the colors indicate a significant association ($p < 0.05$). Abbreviations: abundant bacterial taxa (ABT), moderate bacterial taxa (MBT), rare bacterial taxa (RBT), abundant archaeal taxa (AAT), moderate archaeal taxa (Mattes et al.), and rare archaeal taxa (RAT). T (temperature), ammonium nitrogen (NH_4^+), nitrate nitrogen (NO_3^-), nitrite nitrogen (NO_2^-), dissolved inorganic nitrogen, soluble reactive phosphorus (SRP), silicate (SiO_3^{2-}), dissolved oxygen (DO).

Table 1
Summary of β-diversity components for sub-communities based on Sørensen dissimilarities.

Contribution ratio (%)	TBT	ABT	MBT	RBT	TAT	AAT	MAT	RAT
$\beta_{turn}/\beta_{total}$	79.520	74.495	77.590	56.609	51.532	54.809	56.057	45.023
$\beta_{nest}/\beta_{total}$	20.480	25.505	22.410	43.391	48.468	45.191	43.943	54.977

Abbreviations: abundant bacterial taxa (ABT), moderate bacterial taxa (MBT), rare bacterial taxa (RBT), abundant archaeal taxa (AAT), moderate archaeal taxa (Mattes et al.), and rare archaeal taxa (RAT); β-diversity based on Sørensen dissimilarities (β_{total}), species turnover (β_{turn}), and nestedness (β_{nest}).

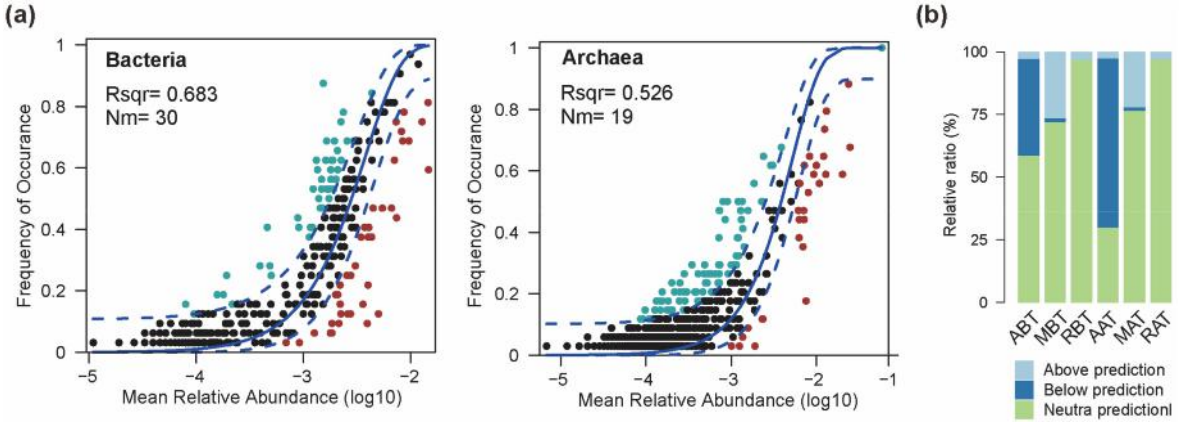

Fig. 3. The NCM appropriateness for the construction of microbial communities in the water column above cold seeps. (a) The estimated occurrence frequency of the bacterial and archaeal communities; (b) ASVs in bacterial and archaeal sub-communities above, within, and below the model fitting. Abbreviations: the same as Fig. 1.

environmental factors (Fig. 3b). For the bacterial community, most of the abundant (58.58%), intermediate (71.85%), and rare (96.61%) ASVs were distributed within the neutral community model. The abundant (3.03% ASVs), moderate (26.66% ASVs), and rare ASVs (3.38% ASVs) were above the prediction of the neutral model, and the taxa below the neutral model were mainly members of the abundant (38.38% ASVs), moderate (1.48% ASVs), and rare ASVs (0% ASVs). For the archaeal community, the abundant (29.72%), moderate (76.32%), and rare (96.90%) ASVs were distributed within the prediction limits, and the abundant (2.70% ASVs), intermediate (22.22% ASVs) and rare OTUs (3.09% ASVs) ranged beyond the neutral model, and the taxa that were below the neutral model mainly belonged to abundant (67.56% ASVs),

moderate (1.44% ASVs), and rare (0% ASVs).

The estimated microbial community niche breadth index revealed the profiles of dispersal limitation and species sorting and their effects on sub-communities. Our results showed that the mean NBI values were significantly higher in the bacterial community compared with the archaeal community (Fig. S7). For bacterial and archaeal sub-communities, the order of magnitude of mean NBI values was abundant taxa, moderate taxa, and rare taxa (Fig. S7).

3.6. Co-occurrence microbial networks

The co-occurrence network included 180 nodes and 1701 edges (Table S3). Most of the edges were positive rather than negative. The modularity, average path length, and average clustering coefficient were higher than Erdös–Réyni random networks, indicating that the network had a non-random structure (Table S3). Abundant and moderate ASVs dominated the nodes of the network (Fig. 4b). The module connectors of the network were affiliated with the bacterial taxa (Gammaproteobacteria) and archaeal taxa (Nitrosopumilaceae and Marine Group II) (Fig. S8, Table S4). The network was divided into six major modules (Fig. 4c); modules 1, 2, and 4 accounted for 25%, 35.55%, and 19.44% of the network nodes, respectively. The results showed that most of the ASVs from module 1 were Nitrosopumilaceae, while modules 3, 4, and 5 were dominated by Gammaproteobacteria. Module 2, composed of substantially abundant ASVs, belonged to Marine Methylotrophic Group 2, *Methylotenera*, *Cycloclasticus*, and SUP05 cluster (Fig. 4d).

3.7. Functional characteristics in the water column of cold seeps

The present study focused on the functional pathways involved in methane oxidation, nitrogen, and sulfur cycles along the depth profile. The stress factor of NMDS was 0.0362, which ensures the NMDS reliability results (Fig. S9). The results of NMDS showed no significant differences in the functional composition of microorganisms at different depths ($P > 0.05$). However, further ANOSIM analysis showed that the functional composition of microorganisms at 1400 m was significantly different ($P < 0.05$) from that in the upper water (400 m,600 m, 1000 m) (Table S5).

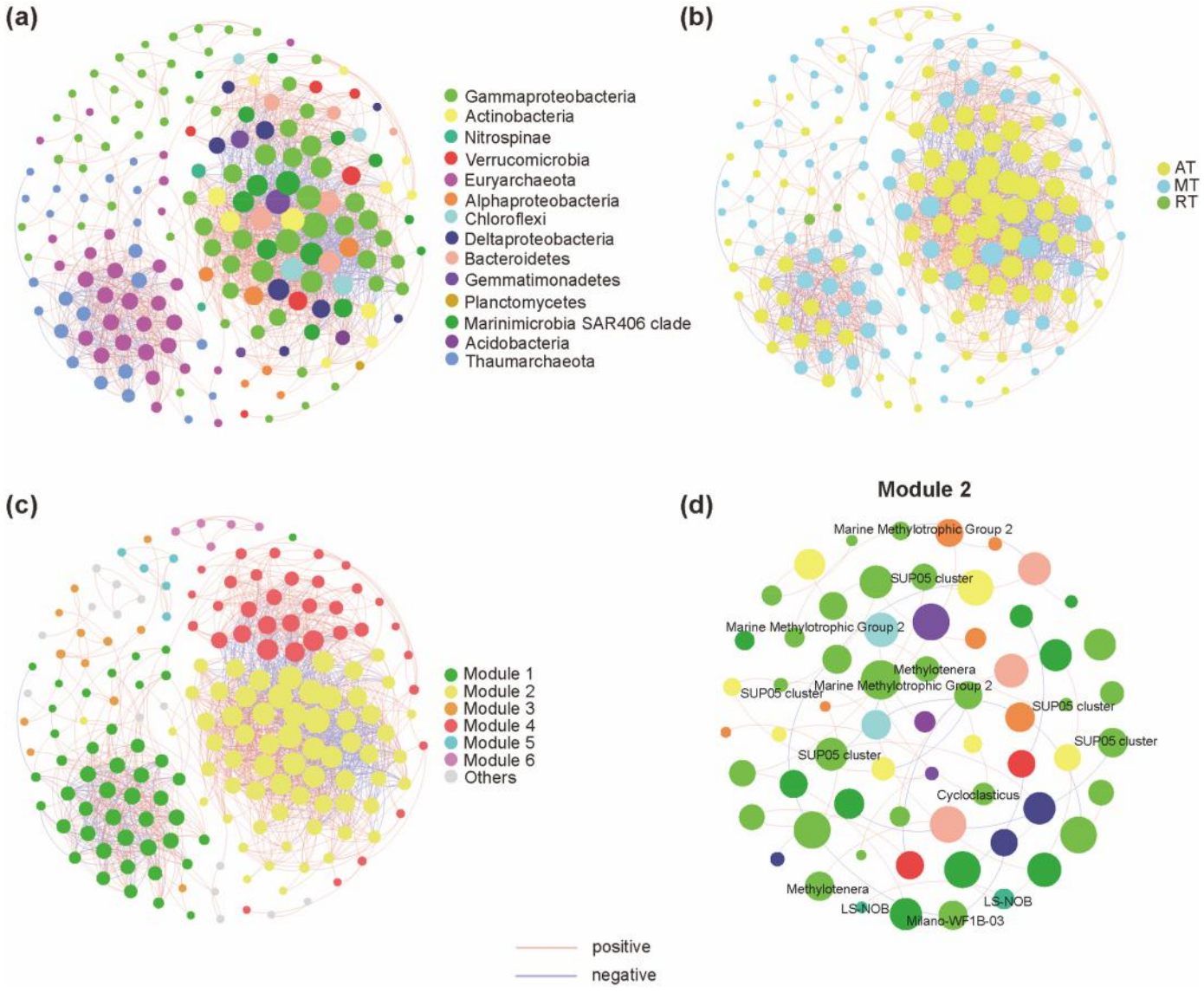

Fig. 4. An overview of microbial co-occurrence network in the cold seep water columns. Positive interactions are exhibited by red edges, whereas negative interactions are exhibited by blue edges. (a) Node colors indicate the bacterial and archaeal phylum of the ASVs; (b) Node colors reveal sub-communities with varying abundances; (c) Modules with more than five nodes are displayed; (d) Module 2 in the co-occurrence network. Abbreviations: abundant taxa (AT), moderate taxa (MT), and rare taxa (RT).

Many genes involved in hydrocarbon and sulfide oxidation exhibit enrichment in the bottom water. For methane metabolism, the gene *mcr* was detected in the bottom water and correlated with methane leakage (Fig. 5a). For nitrogen cycles, the gene *nifH* of nitrogen fixation was the most abundant at a depth of 1400 m (Fig. 5b). Additionally, the genes *nosZ*, *nirS*, and *nirK* that encode denitrification accumulated in the water column of cold seeps (Fig. 5b). For sulfur oxide metabolism, the genes *sox*, *fcc*, and *sqr* exhibited a gradual increase in the trend along with depth gradient, especially in the bottom water (Fig. 5c).

Microbial functional features were highly associated with environmental factors in the water column of cold seeps. The same environmental factors influenced functional traits that catalyzed the same path. For instance, the *mxaCLD* genes involved in methane metabolism were mainly influenced by several environmental factors, such as NH_4^+, NO_3^-, SRP, SiO_3^{2-}, and salinity (Fig. 5d). The *mcrABG* genes were mainly correlated with NO_3^-, SiO_3^{2-}, and salinity (Fig. 5d). The *nosZ* gene showed that all factors were correlated with it except NO_2^- (Fig. 5e). Furthermore, SRB, SiO_3^{2-}, and salinity negatively connected with sulfide reduction pathways (*aprAB*, *dsrAB*), but sulfide oxidation routes (*fccAB*, *sqr*) were positively correlated with those parameters (Fig. 5f). SOX system of sulfur metabolism was significantly correlated with oxygen concentration (Fig. 5f).

In the functional network, it included 35 nodes, 242 edges, and 13.8 average degree (Fig. S10). All of the edges were positive links. The nodes related to nitrogen fixation in the nitrogen cycle exhibit higher degree (including *narG*: 18 and *narH*: 16), while the *nifH* gene does not show significant correlations with other genes. While in the sulfur cycle, nodes related to the SOX system exhibit higher degree (including *soxB*: 21, *soxC*: 23, *soxY*: 20, *soxZ*: 21). Meanwhile, in methane metabolism-related genes, *fmdA* (18), *fmdB* (20), and *fmdC* (15) show higher degree (Table S6). In the functional network, nitrogen fixation processes, the SOX system, and methane metabolism processes exhibit close connections.

4. Discussion

4.1. Species turnover contributes to the β-diversity patterns of bacteria, while archaea exhibit a relatively higher nestedness pattern

Prokaryotic microbial β-diversity not only describes the biogeographic distributions but also provides fundamental insights into assembly mechanisms along environmental gradients (Lindh et al., 2017; Zhang et al., 2020b). The results obtained in this study showed that the bacterial communities exhibited depth stratification (Fig. 1c, Table S2), consistent with previous studies (Lindh et al., 2017; Sunagawa et al., 2015; Zhang et al., 2020c). In contrast, there were no significant differences in archaeal community structures along the depth gradient (Fig. 1c, Table S2), suggesting that archaeal community compositions were more stable compared to bacteria, similar to earlier research (Zhang et al., 2020c). Our results highlight the disparities between bacterial and archaeal community β-diversity patterns in the water column above cold seep.

We found that bacteria showed a relatively higher species turnover (Fig. 2a, Fig. S5), which is consistent with previous studies of environmental gradients (Ren et al., 2022; Shen et al., 2020; Wu et al., 2020). It is widely accepted that species turnover reflects the gains and losses of species between sites as a result of environmental sorting and/or geographic barrier restrictions (Aho et al., 2019; Gaston et al., 2007; Gianuca et al., 2017). The high species turnover of bacterial β-diversity also shows a role in evolutionary adaptation to environmental factors along depth gradient (Qian et al., 2011; Tobias-Hunefeldt et al., 2019; Wu et al., 2020). Unlike bacteria, archaea showed a relatively higher nestedness pattern in this study, although the percentage of nestedness pattern and species turnover were similar (Fig. 2a, Fig. S5). This could be because bacteria and archaea differ greatly in key traits including nutritional state, body size, and dispersal ability (DeLong, 2020). In contrast to species turnover, nestedness implies a different pattern of richness in which the species at a distinct location are a subset of the assemblages at a species-rich site (Baselga, 2010; Mori et al., 2018). The nestedness pattern can be caused by a variety of biological mechanisms, including habitat nestedness, selective colonization or extinction, and interspecific variation in environmental tolerance (Baselga, 2010; Wang et al., 2017a). The findings of our investigation demonstrated that the partitioning of β-diversity in the water column above cold seep was taxonomic dependency (bacteria and archaea).

Our results reveal that depth, temperature, and salinity were the major drivers of the bacterial species turnover pattern by partial Mantel tests (Fig. 2b), which refers to the selection of taxa based on environmental circumstances within the deep-sea (Maloufi et al., 2016; Rasmussen et al., 2021; Wu et al., 2020). Seawater depth is important in defining ocean environmental characteristics such as temperature, nutrient availability, and hydrostatic pressure, all of which have been found to influence bacteria distribution (Sunagawa et al., 2015). Meanwhile fluids discharged from cold seeps drastically affect the physicochemical features of the underlying deep sea along the depth gradient (Wei et al., 2020). Fluid seepage is an important driving factor for bacteria in the water column. It has a direct impact on bacterial diversity by carbon and sulfur electron donors (Orcutt et al., 2011; Vigneron et al., 2014). Although it has already been demonstrated that habitat heterogeneity of the water column above cold seeps contributes to the bacterial β-diversity (Huang et al., 2023; Zhang et al., 2020c), our results provide a new perspective that species turnover of bacteria strongly related to changes in environmental gradients. Furthermore, the change in β-diversity partitioning cannot be explained by ocean depth (Fig. 2b), indicating the pattern of archaeal β-diversity is not restricted by depth. The nestedness pattern of archaea was mainly driven by SRP and SiO_3^{2-} in this study (Fig. 2b), which suggests that the SRP and SiO_3^{2-} in the dark ocean may affect the richness of archaea to some extent. For bacterial and archaeal communities, the species turnover and nestedness components of β-diversity are affected by different ecological mechanisms and thus generally associated with different environmental properties (Lynch and Neufeld, 2015). Along the depth gradient, there are significant differences in associated environmental parameters (temperature, salinity, oxygen, nutrients), which may interact to explain β-diversity patterns.

4.2. Abundant groups showed a higher percentage species turnover pattern than rare groups

Determining the partitioning β-diversity and driving factors of abundant and rare microbial taxa is useful for understanding the maintenance of community structures and ecosystem management (Baselga, 2010; Maloufi et al., 2016). Our results showed that the abundant groups of bacteria and archaea were mainly driven by species turnover, whereas the rare groups showed a higher percentage of nestedness pattern (Fig. 2a). This highlights unique characteristics of different abundance prokaryotic microorganisms that determine the generation and maintenance of microbial biodiversity (Lindh et al., 2017; Lynch and Neufeld, 2015). The reasons for this pattern of differences were that taxa with differential abundances possess distinct properties, such as environmental adaptability, energy requirements, and dispersal ability (Pascoal et al., 2021). These results were similar to a previous study that assessed the microbial communities, in which the contrasting partitioning of microbial β-diversity of taxa with different abundances (Ren et al., 2022; Shen et al., 2020; Xue et al., 2018). The niche theory shows that microbial community diversity is determined by environmental selection and microbial interactions (Benson, 2005). Taxa with varying abundances filled diverse ecological niches and so exhibited distinct distributional patterns (Liu et al., 2019). The ecological tolerance and niche breadth of taxa are crucial factors for species turnover ratio (Leprieur et al., 2011; Wu et al., 2017), which accounts for the higher species turnover ratio of abundant taxa compared to rare

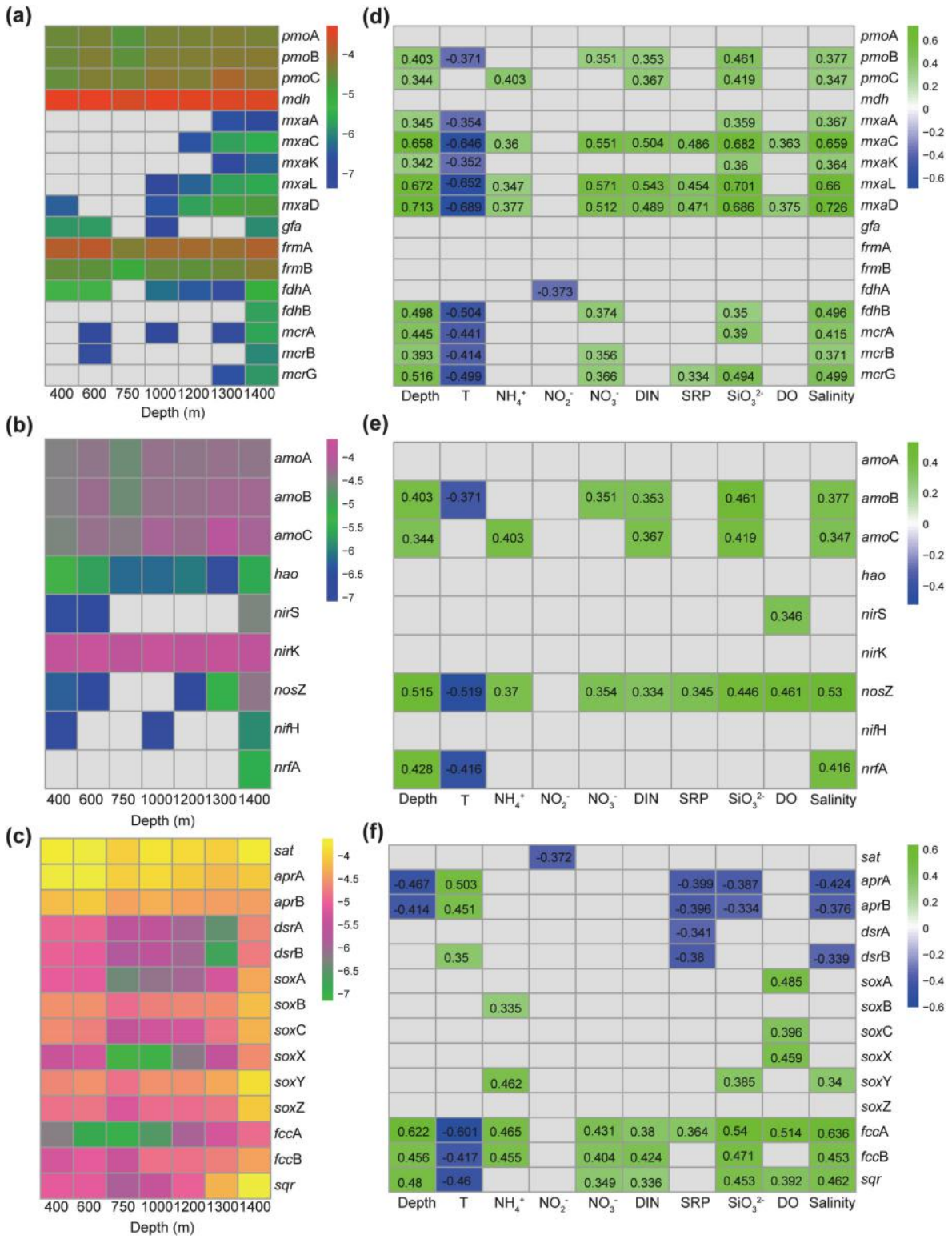

Fig. 5. Heatmaps a, b, and c depict the relative abundance of functional genes engaged in methane, nitrogen, and sulfur cycling across varying depth gradients. The color spectrum signifies different levels of relative abundance. Heatmaps d, e, and f visually represent the relationships between functional genes and local environmental factors. The presence of gray shading indicates the absence of a significant correlation. In contrast, squares filled with green or blue denote a substantial correlation ($p < 0.05$), the green fill corresponds to a positive correlation, while the blue indicates a negative correlation. The depth of color corresponds to the strength of the correlation coefficient which were also noted in the squares. The abbreviations used are consistent with those provided in Fig. 2.

taxa, given their higher niche width (Fig. S7) and ecological tolerance of abundant taxa (Mikulyuk et al., 2017). When considering the lack of resource inputs in deep-sea environments (Orcutt et al., 2011), abundant taxa were more dominant in the competition for resources and therefore more subject to environmental filtering. Microorganisms with differential abundances play different roles in interaction relationships, which influence the microbial β-diversity by altering the numerical abundance of individuals or species in a community (Pedros-Alio, 2006).

Moreover, our results showed that the *β*-diversity pattern (species turnover) and the corresponding environmental drivers (mainly depth, temperature, and salinity) were consistent between the abundant bacterial sub-community and the whole bacterial community (Fig. 2b). However, the *β*-diversity pattern (nestedness) and the corresponding environmental drivers (SRP and SiO_3^{2-}) of *β*-diversity of the rare archaeal sub-community and whole archaeal community were consistent (Fig. 2b). SRP and SiO_3^{2-} may have a greater influence on the richness of rare archaea, which contributes more to the nestedness pattern in the overall archaeal community.

4.3. Abundant taxa were more affected by the deterministic processes than rare taxa

Assembly processes of the microbial community are crucial for ecosystem stability, diversity, and versatility, and determining the impacts of deterministic and stochastic processes is useful for understanding the marine microbial community characteristics (Baselga, 2010; Morrison-Whittle and Goddard, 2015). Our results revealed that stochastic processes play a prominent role in driving the whole bacterial and archaeal community assembly (Fig. 3a), which suggests that the dispersal of bacteria and archaea between the interconnected water layers may be largely random. Fluid released from the cold seep may have driven the bacteria upward, reducing dispersal limitation. Furthermore, we found abundant bacterial and archaeal taxa were more affected by the deterministic processes than rare taxa (Fig. 3b). This result was confirmed by a study revealing that abundant taxa were more determined by deterministic processes than rare taxa in the Western Subtropical Pacific Ocean (Shao et al., 2022). Another study has found that abundant taxa were more influenced by stochastic processes than rare taxa in the surface layer of seawater (Wu et al., 2017). These differences in abundant taxa assembling processes are likely to be dependent on the characterization of the habitats.

Meanwhile, our analysis of VPA showed that temperature combined with nutrients were the main driving factors for the variability of abundant bacterial taxa (Fig. S3c). However, these factors can only explain a very low percentage of the variation in abundant archaeal communities (Fig. S3c), suggesting some unmeasured environmental factors may drive abundant archaeal community assembly. Temperature is an important limiting factor in the marine environment, and several studies have found the effect of temperature on bacterial community assembly (Sunagawa et al., 2015; Zhang et al., 2020c). The effects of nutrients on bacterial communities may be related to the lack of material inputs in deep-sea environments (Orcutt et al., 2011). Given that abundant taxa have broader niche breadths than rare taxa (Fig. S7), it is highly likely that non-neutral processes such as competition, predation, mutualism, and environmental filtering have a larger impact on habitat generalists (wide niche breadth) than on specialists (narrow niche breadth) (Tobias-Hunefeldt et al., 2019; Xia et al., 2017). This could be because abundant and rare taxa have differing environmental sensitivity (Lynch and Neufeld, 2015; Zhang et al., 2018). In addition, rare species had a lower reaction to environmental influences due to their limited population size, rendering them more vulnerable to ecological drift (stochastic processes) (Liu et al., 2019).

4.4. Strong carbon, sulfur, and nitrogen cycles coupling in the bottom water

We found that the distribution pattern of functional taxa related to the biogeochemical cycles revealed a gradient distribution pattern (Fig. 5), suggesting niche partitioning. This is consistent with other studies, which showed that functional taxa concerning carbon, nitrogen, and sulfur metabolism exhibited significant ecological niche differentiation characteristics along a depth gradient (Li et al., 2018; Mayr et al., 2020). Furthermore, the functional pathways involved in the sulfur cycle, methane metabolism, and nitrogen cycle along the depth profile were analyzed to further explore microbial functional components in the water column overlaying cold seep.

For the sulfur cycle, *Sulfurovum* and SUP05 clusters were involved in sulfur oxidation in the water column above the cold seep, but exhibited different distributional characteristics (Fig. S2c). The two ASVs associated with the *Sulfurovum* (ASV_194 and ASV_64) were significantly enriched at 1400 m (Fig. S2c). This may be due to the influence of leakage of cold seep sulfide, especially its role as an important electron donner driving functional microbial community diversity and structure (Mattes et al., 2013; van Vliet et al., 2021). The abundances of several genes involved in the SOX system of sulfur metabolism did not correlate with depth but with oxygen concentration (Fig. 5). Although studies have shown that the SOX genes can couple nitrate metabolism (Wright et al., 2012), the SOX system (*soxA*, *soxC*, and *soxX*) may have a preference for oxygen as an electron acceptor with significantly decreased abundances in the hypoxic zone (750 m–1000 m). Moreover, the *fcca*, *fccb*, *sqr* also exhibited elevated characteristics at the bottom of the water column (Fig. 5) and had similar effect factors. The SQR enzyme and FccAB were related to the oxygen-dependent sulfide oxidation processes (Li et al., 2021b).

For the carbon cycle, we found that *Cycloclasticus* (ASV_424) was only present from 1200 m to 1400 m (Fig. S2c). It has been shown that involved in hydrocarbon degradation (Hernandez-Lopez et al., 2019). In addition, Marine Methylotrophic Group 2 (ASV_24, ASV_276, ASV_293, ASV_86), Milano-WF1B-03 (ASV_73), which exhibited enrichment in the bottom water (Fig. S2c), and involved in methane oxidation (Kalyuzhnaya et al., 2012; Rubin-Blum et al., 2019; Unger et al., 2021). Methane oxidation is one of the most common carbon cycle processes in cold seeps, and it is primarily driven by two taxa, aerobic methane-oxidizing bacteria, and anaerobic methane-oxidizing archaea (Cheng et al., 2022; Vigneron et al., 2014). Previous studies have found that methane depletion in cold seep sediments was dominated by anaerobic methane-oxidizing archaea (Ruff et al., 2015). However, our results showed a considerable enrichment of aerobic methane-oxidizing bacteria in bottom water, but anaerobic methane-oxidizing archaea did not show significant enrichment in bottom water, owing to enhanced dissolved oxygen in bottom water, which is more conducive for aerobic organism metabolism (Cheng et al., 2022). There is an increasing consensus that the methane concentration in the water column is closely related to the cold seep activity, which subsequently influences nutrient metabolism and functional activity rates (Lv et al., 2022; Suess, 2014). The accumulation of hydrocarbon and sulfide oxidation-related genes suggests that microbes generate chemical energy through oxidizing methane and hydrogen sulfide to support the primary productivity in the bottom water. It has been reported that microbes possessing hydrocarbon oxidation genes may act as a sequester methane (Savvichev et al., 2018), and microbes capable of hydrogen sulfide oxidation play an important role in reducing the toxicity of hydrogen sulfide to other organisms.

For the nitrogen cycle, the LS-NOB was observed at a depth ranging from 400 m to 1200 m and gradually decreased in abundance (Fig. S2c). NOB obtains energy through nitrite oxidation in the energy-limited dark ocean while participating in the process of deep-sea carbon fixation (Zhang et al., 2020d). Denitrification-related genes *nirS*, *nirK*, and *nosZ* exhibited higher relative abundance at the bottom water (Fig. 5),

suggesting that the water column above cold seeps may be potential sources and sinks for nitrous oxide. Denitrification processes were often coupled with other electron donor oxidation processes, such as sulfur oxidation, and methane oxidation (Jing et al., 2020; Li et al., 2021b). Furthermore, the nitrogen-fixing-related gene *nifH* was also enriched at the bottom water (Fig. 5), and the nitrogen-fixing process is energy-dependent (Dong et al., 2022; Metcalfe et al., 2021). Previous studies have identified the diversity and abundance of nitrogen-fixing microorganisms (diazotrophs) in the cold seep sediments (Dong et al., 2022), suggesting an impact on the deep-sea nitrogen cycle. The energy produced by hydrogen sulfide oxidation and methane oxidation processes may provide an energy source for the nitrogen-fixing process (Metcalfe et al., 2021), which implies the coupling of carbon and nitrogen cycles in the bottom water.

Some of functional genes that participated in denitrification, sulfur oxidation, and methane oxidation were significantly correlated with water depth and NO_3^- (Fig. 5). Nitrate acted as an important electron acceptor simultaneously affecting gradient changes in multiple functional genes, suggesting that oxidizing electron donors such as methane and sulfide was closely related to the nitrate reduction processes (Li et al., 2021b; Orcutt et al., 2011). It has been shown that some methane-oxidizing and sulfur-oxidizing microorganisms have both denitrification genes (Cheng et al., 2022; Shao et al., 2010), which is one reason why the relevant genes are simultaneously associated with nitrate with increasing depth.

We further found that the biomarker Marine Methylotrophic Group 2 and other groups, including *Methylotenera*, *Cycloclasticus*, and SUP05, clustered in a common network module (module 2) (Fig. 4d), which were involved in methane and sulfide oxidation processes (Callbeck et al., 2018; Hernandez-Lopez et al., 2019; Kalyuzhnaya et al., 2012). It has been shown that microorganisms in the same network module are potentially more closely linked in their habitats (Shi et al., 2020). This statistical network relationship suggests a possible coupling between hydrogen sulfide oxidation and methane oxidation, which supports the hypothesis that the coupling metabolism of sulfate and methane may occur among microorganisms through the linkage of oxidizing hydrogen sulfide to sulfate (Lv et al., 2022). As found in our study, these functional taxa were significantly enriched in the bottom water above cold seep (Fig. S2c). Furthermore, functional network analysis was used to reveal the potential relevance concerning denitrification, sulfur oxidation, and methane oxidation (Fig. S10). Thus, the synthesis of these results presumably suggests that cold seep potentially enhanced bottom water carbon, nitrogen, and sulfur cycle coupling. Our results suggest that functional taxa enriched in the water column above cold seeps, on the one hand, reinforced previous understanding of the influence of cold seep fluids on the geochemical cycling of the water column (Dong et al., 2022; Jing et al., 2020), and on the other hand, indicated that bottom-enriched microorganisms exhibited a tendency to spread to higher water layers, and thus that cold seeps acted as a seed bank for some functional microorganisms to influence the geochemical cycling processes of the surrounding waters more broadly (Ruff et al., 2015).

5. Conclusions

Herein, we found divergent β-diversity patterns and assembly mechanisms of the microbial sub-communities in the water column of deep-sea cold seeps. The β-diversity of the bacterial community was mainly explained by the species turnover pattern, while the archaeal community showed a higher percentage of nestedness pattern. The depth and local factors accounted for most of the variations in patterns of β-diversity components for the bacterial community, and the nestedness pattern of the archaeal community was mainly driven by soluble reactive phosphate and SiO_3^{2-}. The β-diversity patterns of abundant and rare taxa differed, with deterministic processes playing a more significant role in shaping the β-diversity of abundant taxa than rare taxa. The metagenomics results provided further evidence of the effects of seepage on methane oxidation, sulfur oxidation, and nitrogen fixation processes in the water column around cold seeps. Overall, we emphasize the distinct environmental distribution patterns and assembly mechanisms of abundant and rare prokaryotic microorganisms, which will help to understand the microbial responses to seepages in the dark ocean more comprehensively.

CRediT authorship contribution statement

Y.J. Lyu: Investigation, Formal Analysis, Writing - Original Draft; J. Zhang: Investigation, Formal Analysis, Writing; Y. Chen: Resources and sampling, Investigation; Q.Q. Li: Resources and sampling, Investigation; Z.X. Ke: Investigation; S. Zhang: Funding Acquisition, Supervision; J. Li: Conceptualization, Funding Acquisition, Resources, Supervision, Writing - Review & Editing.

Declaration of competing interest

The authors declare that they have no known competing financial interests or personal relationships that could have appeared to influence the work reported in this paper.

Data availability

I have shared the link to my data in the manuscript.

Acknowledgments

We are very grateful to the crew of the Haiyang Dizhi 6 ship and the operation team members of Haima ROV for their great support in sampling. This research was funded by the Guangdong Major Project of Basic and Applied Basic Research (2019B030302004), and Scientific Instrument Developing Project of the Chinese Academy of Sciences, Grant No. YJKYYQ20210015, and the development fund of South China Sea Institute of Oceanology of the Chinese Academy of Sciences (SCSIO202202).

Appendix A. Supplementary data

Supplementary data to this article can be found online at https://doi.org/10.1016/j.jenvman.2023.119240.

References

Aho, K.A., Weber, C.F., Christner, B.C., Vinatzer, B.A., Morris, C.E., Joyce, R., Failor, K. C., Werth, J.T., Bayless-Edwards, A.L.H., Schmale, D.G., 2019. Spatiotemporal patterns of microbial composition and diversity in precipitation. Ecol. Monogr. 90 (1) https://doi.org/10.1002/ecm.1394.

Baselga, A., 2010. Partitioning the turnover and nestedness components of beta diversity. Global Ecol. Biogeogr. 19 (1), 134–143. https://doi.org/10.1111/j.1466-8238.2009.00490.x.

Benson, K.R., 2005. Ecological niches: linking classical and contemporary approaches. Hist. Philos. Life Sci. 27 (2), 304–305. Go to ISI>://WOS:000236941900021.

Boetius, A., Wenzhofer, F., 2013. Seafloor oxygen consumption fuelled by methane from cold seeps. Nat. Geosci. 6 (9), 725–734. https://doi.org/10.1038/ngeo1926.

Bolyen, E., Rideout, J.R., Dillon, M.R., Bokulich, N.A., Abnet, C.C., Al-Ghalith, G.A., Alexander, H., Alm, E.J., Arumugam, M., Asnicar, F., Bai, Y., Bisanz, J.E., Bittinger, K., Brejnrod, A., Brislawn, C.J., Brown, C.T., Callahan, B.J., Caraballo-Rodriguez, A.M., Chase, J., Cope, E.K., Da Silva, R., Diener, C., Dorrestein, P.C., Douglas, G.M., Durall, D.M., Duvallet, C., Edwardson, C.F., Ernst, M., Estaki, M., Fouquier, J., Gauglitz, J.M., Gibbons, S.M., Gibson, D.L., Gonzalez, A., Gorlick, K., Guo, J., Hillmann, B., Holmes, S., Holste, H., Huttenhower, C., Huttley, G.A., Janssen, S., Jarmusch, A.K., Jiang, L., Kaehler, B.D., Kang, K.B., Keefe, C.R., Keim, P., Kelley, S.T., Knights, D., Koester, I., Kosciolek, T., Kreps, J., Langille, M.G.I., Lee, J., Ley, R., Liu, Y.X., Loftfield, E., Lozupone, C., Maher, M., Marotz, C., Martin, B.D., McDonald, D., McIver, L.J., Melnik, A.V., Metcalf, J.L., Morgan, S.C., Morton, J.T., Naimey, A.T., Navas-Molina, J.A., Nothias, L.F., Orchanian, S.B., Pearson, T., Peoples, S.L., Petras, D., Preuss, M.L., Pruesse, E., Rasmussen, L.B., Rivers, A., Robeson 2nd, M.S., Rosenthal, P., Segata, N., Shaffer, M., Shiffer, A., Sinha, R., Song, S.J., Spear, J.R., Swafford, A.D., Thompson, L.R., Torres, P.J., Trinh, P., Tripathi, A., Turnbaugh, P.J., Ul-Hasan, S., van der Hooft, J.J.J., Vargas, F., Vazquez-Baeza, Y., Vogtmann, E., von Hippel, M., Walters, W., Wan, Y., Wang, M., Warren, J.,

Weber, K.C., Williamson, C.H.D., Willis, A.D., Xu, Z.Z., Zaneveld, J.R., Zhang, Y., Zhu, Q., Knight, R., Caporaso, J.G., 2019. Author Correction: reproducible, interactive, scalable and extensible microbiome data science using QIIME 2. Nat. Biotechnol. 37 (9), 1091. https://doi.org/10.1038/s41587-019-0252-6.

Callahan, B.J., McMurdie, P.J., Rosen, M.J., Han, A.W., Johnson, A.J.A., Holmes, S.P., 2016. DADA2: high-resolution sample inference from Illumina amplicon data. Nat. Methods 13 (7), 581. https://doi.org/10.1038/nmeth.3869.

Callbeck, C.M., Lavik, G., Ferdelman, T.G., Fuchs, B., Gruber-Vodicka, H.R., Hach, P.F., Littmann, S., Schoffelen, N.J., Kalvelage, T., Thomsen, S., Schunck, H., Loscher, C.R., Schmitz, R.A., Kuypers, M.M.M., 2018. Oxygen minimum zone cryptic sulfur cycling sustained by offshore transport of key sulfur oxidizing bacteria. Nat. Commun. 9 (1), 1729. https://doi.org/10.1038/s41467-018-04041-x.

Campbell, B.J., Yu, L., Heidelberg, J.F., Kirchman, D.L., 2011. Activity of abundant and rare bacteria in a coastal ocean. Proc. Natl. Acad. Sci. U. S. A. 108 (31), 12776–12781. https://doi.org/10.1073/pnas.1101405108.

Cao, L., Lian, C., Zhang, X., Zhang, H., Wang, H., Zhou, L., Wang, M., Chen, H., Luan, Z., Li, C., 2021. In situ detection of the fine scale heterogeneity of active cold seep environment of the Formosa Ridge, the South China Sea. J. Mar. Syst. 218 https://doi.org/10.1016/j.jmarsys.2021.103530.

Chen, W., Ren, K., Isabwe, A., Chen, H., Liu, M., Yang, J., 2019. Correction to: stochastic processes shape microeukaryotic community assembly in a subtropical river across wet and dry seasons. Microbiome 7 (1), 148. https://doi.org/10.1186/s40168-019-0763-x.

Cheng, C., He, Q., Zhang, J., Chen, B., Pavlostathis, S.G., 2022. Is the role of aerobic methanotrophs underestimated in methane oxidation under hypoxic conditions? Sci. Total Environ. 833, 155244 https://doi.org/10.1016/j.scitotenv.2022.155244.

Cruaud, P., Vigneron, A., Pignet, P., Caprais, J.-C., Lesongeur, F., Toffin, L., Godfroy, A., Cambon-Bonavita, M.-A., 2015. Microbial communities associated with benthic faunal assemblages at cold seep sediments of the Sonora Margin, Guaymas Basin. Front. Mar. Sci. 2 https://doi.org/10.3389/fmars.2015.00053.

DeLong, E.F., 2020. Exploring marine planktonic archaea: then and now. Front. Microbiol. 11, 616086 https://doi.org/10.3389/fmicb.2020.616086.

Deng, Y., Jiang, Y.H., Yang, Y.F., He, Z.L., Luo, F., Zhou, J.Z., 2012. Molecular ecological network analyses. Bmc Bioinformat. 13, 113. https://doi.org/10.1186/1471-2105-13-113.

Dinghua, L., Chi-Man, L., Ruibang, L., Kunihiko, S., Tak-Wah, L., 2015. MEGAHIT: an ultra-fast single-node solution for large and complex metagenomics assembly via succinct de Bruijn graph. Bioinformatics 31 (10), 1674–1676.

Dini-Andreote, F., Stegen, J.C., van Elsas, J.D., Salles, J.F., 2015. Disentangling mechanisms that mediate the balance between stochastic and deterministic processes in microbial succession. Proc. Natl. Acad. Sci. U.S.A. 112 (11), E1326–E1332. https://doi.org/10.1073/pnas.1414261112.

Dong, X., Zhang, C., Peng, Y., Zhang, H.X., Shi, L.D., Wei, G., Hubert, C.R.J., Wang, Y., Greening, C., 2022. Phylogenetically and catabolically diverse diazotrophs reside in deep-sea cold seep sediments. Nat. Commun. 13 (1), 4885. https://doi.org/10.1038/s41467-022-32503-w.

Feng, D., Qiu, J.-W., Hu, Y., Peckmann, J., Guan, H., Tong, H., Chen, C., Chen, J., Gong, S., Li, N., Chen, D., 2018. Cold seep systems in the South China Sea: an overview. J. Asian Earth Sci. 168, 3–16. https://doi.org/10.1016/j.jseaes.2018.09.021.

Feng, J.-C., Yang, Z., Zhou, W., Feng, X., Wei, F., Li, B., Ma, C., Zhang, S., Xia, L., Cai, Y., Wang, Y., 2022. Interactions of microplastics and methane seepage in the Deep-Sea environment. Engineering. https://doi.org/10.1016/j.eng.2022.08.009.

Frank, A.H., Garcia, J.A., Herndl, G.J., Reinthaler, T., 2016. Connectivity between surface and deep waters determines prokaryotic diversity in the North Atlantic Deep Water. Environ. Microbiol. 18 (6), 2052–2063. https://doi.org/10.1111/1462-2920.13237.

Gaston, K.J., Davies, R.G., Orme, C.D., Olson, V.A., Thomas, G.H., Ding, T.S., Rasmussen, P.C., Lennon, J.J., Bennett, P.M., Owens, I.P., Blackburn, T.M., 2007. Spatial turnover in the global avifauna. Proc. Biol. Sci. 274 (1618), 1567–1574. https://doi.org/10.1098/rspb.2007.0236.

Gianuca, A.T., Declerck, S.A., Lemmens, P., De Meester, L., 2017. Effects of dispersal and environmental heterogeneity on the replacement and nestedness components of beta-diversity. Ecology 98 (2), 525–533. https://doi.org/10.1002/ecy.1666.

Gurevich, A., Saveliev, V., Vyahhi, N., Tesler, G., 2013. QUAST: quality assessment tool for genome assemblies. Bioinformatics 29 (8), 1072–1075. https://doi.org/10.1093/bioinformatics/btt086.

Hansman, R.L., Thurber, A.R., Levin, L.A., Aluwihare, L.I., 2017. Methane fates in the benthos and water column at cold seep sites along the continental margin of Central and North America. Deep Sea Res. Oceanogr. Res. Pap. 120, 122–131. https://doi.org/10.1016/j.dsr.2016.12.016.

Hernandez-Lopez, E.L., Gasperin, J., Bernaldez-Sarabia, J., Licea-Navarro, A.F., Guerrero, A., Lizarraga-Partida, M.L., 2019. Detection of Alcanivorax spp., Cycloclasticus spp., and Methanomicrobiales in water column and sediment samples in the Gulf of Mexico by qPCR. Environ. Sci. Pollut. Res. Int. 26 (34), 35131–35139. https://doi.org/10.1007/s11356-019-06551-7.

Huang, Y., Feng, J.C., Kong, J., Sun, L., Zhang, M., Huang, Y., Tang, L., Zhang, S., Yang, Z., 2023. Community assemblages and species coexistence of prokaryotes controlled by local environmental heterogeneity in a cold seep water column. Sci. Total Environ. 868, 161725 https://doi.org/10.1016/j.scitotenv.2023.161725.

Hugoni, M., Taib, N., Debroas, D., Domaizon, I., Jouan Dufournel, I., Bronner, G., Salter, I., Agogue, H., Mary, I., Galand, P.E., 2013. Structure of the rare archaeal biosphere and seasonal dynamics of active ecotypes in surface coastal waters. Proc. Natl. Acad. Sci. U. S. A. 110 (15), 6004–6009. https://doi.org/10.1073/pnas.1216863110.

Hyatt, D., LoCascio, P.F., Hauser, L.J., Uberbacher, E.C., 2012. Gene and translation initiation site prediction in metagenomic sequences. Bioinformatics 28 (17), 2223–2230. https://doi.org/10.1093/bioinformatics/bts429.

Jing, H., Wang, R., Jiang, Q., Zhang, Y., Peng, X., 2020. Anaerobic methane oxidation coupled to denitrification is an important potential methane sink in deep-sea cold seeps. Sci. Total Environ. 748, 142459 https://doi.org/10.1016/j.scitotenv.2020.142459.

Kalyuzhnaya, M.G., Beck, D.A.C., Vorobev, A., Smalley, N., Kunkel, D.D., Lidstrom, M.E., Chistoserdova, L., 2012. Novel methylotrophic isolates from lake sediment, description of Methylotenera versatilis sp. nov. and emended description of the genus Methylotenera. Int. J. Syst. Evol. Microbiol. 62 (Pt 1), 106–111. https://doi.org/10.1099/ijs.0.029165-0.

Ke, Z., Li, R., Chen, Y., Chen, D., Chen, Z., Lian, X., Tan, Y., 2022. A preliminary study of macrofaunal communities and their carbon and nitrogen stable isotopes in the Haima cold seeps, South China Sea. Deep Sea Res. Oceanogr. Res. Pap. 184 https://doi.org/10.1016/j.dsr.2022.103774.

Lam, T.Y.C., Mei, R., Wu, Z., Lee, P.K.H., Liu, W.T., Lee, P.H., 2020. Superior resolution characterisation of microbial diversity in anaerobic digesters using full-length 16S rRNA gene amplicon sequencing. Water Res. 178, 115815 https://doi.org/10.1016/j.watres.2020.115815.

Landeiro, V.L., Franz, B., Heino, J., Siqueira, T., Bini, L.M., Ibáñez, I., 2018. Species-poor and low-lying sites are more ecologically unique in a hyperdiverse Amazon region: evidence from multiple taxonomic groups. Divers. Distrib. 24 (7), 966–977. https://doi.org/10.1111/ddi.12734.

Legendre, P., 2014. Interpreting the replacement and richness difference components of beta diversity. Global Ecol. Biogeogr. 23 (11), 1324–1334. https://doi.org/10.1111/geb.12207.

Lennon, J.T., Jones, S.E., 2011. Microbial seed banks: the ecological and evolutionary implications of dormancy. Nat. Rev. Microbiol. 9 (2), 119–130. https://doi.org/10.1038/nrmicro2504.

Leprieur, F., Tedesco, P.A., Hugueny, B., Beauchard, O., Durr, H.H., Brosse, S., Oberdorff, T., 2011. Partitioning global patterns of freshwater fish beta diversity reveals contrasting signatures of past climate changes. Ecol. Lett. 14 (4), 325–334. https://doi.org/10.1111/j.1461-0248.2011.01589.x.

Li, J., Liu, C.-l., Wu, N.-y., Xu, X.-q., Hu, G.-w., Li, Y.-l., Meng, Q.-g., 2022. Identification of functionally active aerobic methanotrophs and their methane oxidation potential in sediments from the Shenhu area, South China Sea. China Geology 5 (2), 1–8. https://doi.org/10.31035/cg2022011.

Li, Y., Jing, H., Xia, X., Cheung, S., Suzuki, K., Liu, H., 2018. Metagenomic insights into the microbial community and nutrient cycling in the western subarctic Pacific Ocean. Front. Microbiol. 9, 623. https://doi.org/10.3389/fmicb.2018.00623.

Li, M., Mi, T., He, H., Chen, Y., Zhen, Y., Yu, Z., 2021a. Active bacterial and archaeal communities in coastal sediments: biogeography pattern, assembly process and co-occurrence relationship. Sci. Total Environ. 750, 142252 https://doi.org/10.1016/j.scitotenv.2020.142252.

Li, W.L., Dong, X., Lu, R., Zhou, Y.L., Zheng, P.F., Feng, D., Wang, Y., 2021b. Microbial ecology of sulfur cycling near the sulfate-methane transition of deep-sea cold seep sediments. Environ. Microbiol. 23 (11), 6844–6858. https://doi.org/10.1111/1462-2920.15796.

Liang, Q., Hu, Y., Feng, D., Peckmann, J., Chen, L., Yang, S., Liang, J., Tao, J., Chen, D., 2017. Authigenic carbonates from newly discovered active cold seeps on the northwestern slope of the South China Sea: constraints on fluid sources, formation environments, and seepage dynamics. Deep Sea Res. Oceanogr. Res. Pap. 124, 31–41. https://doi.org/10.1016/j.dsr.2017.04.015.

Lindh, M.V., Maillot, B.M., Shulse, C.N., Gooday, A.J., Amon, D.J., Smith, C.R., Church, M.J., 2017. From the surface to the Deep-Sea: bacterial distributions across polymetallic nodule fields in the clarion-clipperton zone of the Pacific Ocean. Front. Microbiol. 8, 1696. https://doi.org/10.3389/fmicb.2017.01696.

Liu, J., Meng, Z., Liu, X., Zhang, X.-H., 2019. Microbial assembly, interaction, functioning, activity and diversification: a review derived from community compositional data. Marine Life Science & Technology 1 (1), 112–128. https://doi.org/10.1007/s42995-019-00004-3.

Liu, R., Wang, L., Liu, Q., Wang, Z., Li, Z., Fang, J., Zhang, L., Luo, M., 2018. Depth-resolved distribution of particle-attached and free-living bacterial communities in the water column of the new britain trench. Front. Microbiol. 9, 625. https://doi.org/10.3389/fmicb.2018.00625.

Lv, Y.X., Yang, S.S., Xiao, X., Zhang, Y., 2022. Stimulated organic carbon cycling and microbial community shift driven by a simulated cold-seep eruption. mBio 13 (2), e00087-22. https://doi.org/10.1128/mbio.00087-22.

Lynch, M.D., Neufeld, J.D., 2015. Ecology and exploration of the rare biosphere. Nat. Rev. Microbiol. 13 (4), 217–229. https://doi.org/10.1038/nrmicro3400.

Maloufi, S., Catherine, A., Mouillot, D., Louvard, C., Couté, A., Bernard, C., Troussellier, M., 2016. Environmental heterogeneity among lakes promotes hyper β-diversity across phytoplankton communities. Freshw. Biol. 61 (5), 633–645. https://doi.org/10.1111/fwb.12731.

Mattes, T.E., Nunn, B.L., Marshall, K.T., Proskurowski, G., Kelley, D.S., Kawka, O.E., Goodlett, D.R., Hansell, D.A., Morris, R.M., 2013. Sulfur oxidizers dominate carbon fixation at a biogeochemical hot spot in the dark ocean. ISME J. 7 (12), 2349–2360. https://doi.org/10.1038/ismej.2013.113.

Mayr, M.J., Zimmermann, M., Guggenheim, C., Brand, A., Burgmann, H., 2020. Niche partitioning of methane-oxidizing bacteria along the oxygen-methane counter gradient of stratified lakes. ISME J. 14 (1), 274–287. https://doi.org/10.1038/s41396-019-0515-8.

Metcalfe, K.S., Murali, R., Mullin, S.W., Connon, S.A., Orphan, V.J., 2021. Experimentally-validated correlation analysis reveals new anaerobic methane

oxidation partnerships with consortium-level heterogeneity in diazotrophy. ISME J. 15 (2), 377–396. https://doi.org/10.1038/s41396-020-00757-1.
Mikulyuk, A., Barton, M., Hauxwell, J., Hein, C., Kujawa, E., Minahan, K., Nault, M.E., Oele, D.L., Wagner, K.I., 2017. A macrophyte bioassessment approach linking taxon-specific tolerance and abundance in north temperate lakes. J. Environ. Manag. 199, 172–180. https://doi.org/10.1016/j.jenvman.2017.05.012.
Milke, F., Wagner-Doebler, I., Wienhausen, G., Simon, M., 2022. Selection, drift and community interactions shape microbial biogeographic patterns in the Pacific Ocean. ISME J. 16 (12), 2653–2665. https://doi.org/10.1038/s41396-022-01318-4.
Mori, A.S., Isbell, F., Seidl, R., 2018. Beta-diversity, community assembly, and ecosystem functioning. Trends Ecol. Evol. 33 (7), 549–564. https://doi.org/10.1016/j.tree.2018.04.012.
Morrison-Whittle, P., Goddard, M.R., 2015. Quantifying the relative roles of selective and neutral processes in defining eukaryotic microbial communities. ISME J. 9 (9), 2003–2011. https://doi.org/10.1038/ismej.2015.18.
Newman, M.E.J., 2006. Modularity and community structure in networks. Proc. Nat. Acad. Sci. U. S. A. 103 (23), 8577–8582.
Orcutt, B.N., Sylvan, J.B., Knab, N.J., Edwards, K.J., 2011. Microbial ecology of the dark ocean above, at, and below the seafloor. Microbiol. Mol. Biol. Rev. 75 (2), 361–422. https://doi.org/10.1128/MMBR.00039-10.
Pandit, S.N., Kolasa, J., Cottenie, K., 2009. Contrasts between habitat generalists and specialists: an empirical extension to the basic metacommunity framework. Ecology 90 (8), 2253–2262. https://doi.org/10.1890/08-0851.1.
Pascoal, F., Costa, R., Magalhaes, C., 2021. The microbial rare biosphere: current concepts, methods and ecological principles. FEMS Microbiol. Ecol. 97 (1) https://doi.org/10.1093/femsec/fiaa227.
Pedros-Alio, C., 2006. Marine microbial diversity: can it be determined? Trends Microbiol. 14 (6), 257–263. https://doi.org/10.1016/j.tim.2006.04.007.
Pop Ristova, P., Wenzhöfer, F., Ramette, A., Zabel, M., Fischer, D., Kasten, S., Boetius, A., 2012. Bacterial diversity and biogeochemistry of different chemosynthetic habitats of the REGAB cold seep (West African margin, 3160 m water depth). Biogeosciences 9 (12), 5031–5048. https://doi.org/10.5194/bg-9-5031-2012.
Qian, P.-Y., Wang, Y., Lee, O.O., Lau, S.C.K., Yang, J., Lafi, F.F., Al-Suwailem, A., Wong, T.Y.H., 2011. Erratum: vertical stratification of microbial communities in the Red Sea revealed by 16S rDNA pyrosequencing. ISME J. 5 (3), 568. https://doi.org/10.1038/ismej.2010.159, 568.
Quast, C., Pruesse, E., Yilmaz, P., Gerken, J., Glckner, F.O., 2012. The SILVA ribosomal RNA gene database project: improved data processing and web-based tools. Nucleic Acids Res. 41 (D1).
Rasmussen, A.N., Damashek, J., Eloe-Fadrosh, E.A., Francis, C.A., 2021. In-depth spatiotemporal characterization of planktonic archaeal and bacterial communities in north and South San Francisco bay. Microb. Ecol. 81 (3), 601–616. https://doi.org/10.1007/s00248-020-01621-7.
Ren, Z., Zhang, C., Li, X., Ma, K., Cui, B., 2022. Abundant and rare bacterial taxa structuring differently in sediment and water in thermokarst lakes in the yellow river source area, qinghai-tibet plateau. Front. Microbiol. 13, 774514 https://doi.org/10.3389/fmicb.2022.774514.
Rubin-Blum, M., Antony, C.P., Sayavedra, L., Martinez-Perez, C., Birgel, D., Peckmann, J., Wu, Y.C., Cardenas, P., MacDonald, I., Marcon, Y., Sahling, H., Hentschel, U., Dubilier, N., 2019. Fueled by methane: deep-sea sponges from asphalt seeps gain their nutrition from methane-oxidizing symbionts. ISME J. 13 (5), 1209–1225. https://doi.org/10.1038/s41396-019-0346-7.
Ruff, S.E., Biddle, J.F., Teske, A.P., Knittel, K., Boetius, A., Ramette, A., 2015. Global dispersion and local diversification of the methane seep microbiome. Proc. Natl. Acad. Sci. U. S. A. 112 (13), 4015–4020. https://doi.org/10.1073/pnas.1421865112.
Savvichev, A.S., Kadnikov, V.V., Kravchishina, M.D., Galkin, S.V., Novigatskii, A.N., Sigalevich, P.A., Merkel, A.Y., Ravin, N.V., Pimenov, N.V., Flint, M.V., 2018. Methane as an organic matter source and the trophic basis of a laptev sea cold seep microbial community. Geomicrobiol. J. 35 (5), 411–423. https://doi.org/10.1080/01490451.2017.1382612.
Schreiber, L., Holler, T., Knittel, K., Meyerdierks, A., Amann, R., 2010. Identification of the dominant sulfate-reducing bacterial partner of anaerobic methanotrophs of the ANME-2 clade. Environ. Microbiol. 12 (8), 2327–2340. https://doi.org/10.1111/j.1462-2920.2010.02275.x.
Shao, M.F., Zhang, T., Fang, H.H., 2010. Sulfur-driven autotrophic denitrification: diversity, biochemistry, and engineering applications. Appl. Microbiol. Biotechnol. 88 (5), 1027–1042. https://doi.org/10.1007/s00253-010-2847-1.
Shao, Q., Sun, D., Fang, C., Feng, Y., Wang, C., 2022. Biodiversity and biogeography of abundant and rare microbial assemblages in the western subtropical Pacific Ocean. Front. Microbiol. 13 https://doi.org/10.3389/fmicb.2022.839562.
Shen, C., Gunina, A., Luo, Y., Wang, J., He, J.Z., Kuzyakov, Y., Hemp, A., Classen, A.T., Ge, Y., 2020. Contrasting patterns and drivers of soil bacterial and fungal diversity across a mountain gradient. Environ. Microbiol. 22 (8), 3287–3301. https://doi.org/10.1111/1462-2920.15090.
Shi, Y., Delgado-Baquerizo, M., Li, Y., Yang, Y., Zhu, Y.G., Penuelas, J., Chu, H., 2020. Abundance of kinless hubs within soil microbial networks are associated with high functional potential in agricultural ecosystems. Environ. Int. 142, 105869 https://doi.org/10.1016/j.envint.2020.105869.
Sloan, W.T., Lunn, M., Woodcock, S., Head, I.M., Nee, S., Curtis, T.P., 2006. Quantifying the roles of immigration and chance in shaping prokaryote community structure. Environ. Microbiol. 8 (4), 732–740. https://doi.org/10.1111/j.1462-2920.2005.00956.x.
Sogin, M., Morrison, H., Huber, J., Welch, D., Huse, S., Neal, P., Arrieta, J., Herndl, G., 2006. Microbial diversity in the deep sea and the underexplored "rare biosphere". Proc. Natl. Acad. Sci. USA 103 (32), 12115–12120.
Song, W., Liu, J.H., Qin, W., Huang, J., Yu, X.L., Xu, M.Z., Stahl, D., Jiao, N.Z., Zhou, J.Z., Tu, Q.C., 2022. Functional traits resolve mechanisms governing the assembly and distribution of nitrogen-cycling microbial communities in the global ocean. mBio 13 (2), e03832-21. https://doi.org/10.1128/mbio.03832-21.
Specziár, A., Árva, D., Tóth, M., Móra, A., Schmera, D., Várbíró, G., Erős, T., 2018. Environmental and spatial drivers of beta diversity components of chironomid metacommunities in contrasting freshwater systems. Hydrobiologia 819 (1), 123–143. https://doi.org/10.1007/s10750-018-3632-x.
Steinegger, M., Söding, J., 2017. MMseqs2 enables sensitive protein sequence searching for the analysis of massive data sets. Nat. Biotechnol. 35 (11), 1026–1028. https://doi.org/10.1038/nbt.3988.
Suess, E., 2014. Marine cold seeps and their manifestations: geological control, biogeochemical criteria and environmental conditions. Int. J. Earth Sci. 103 (7), 1889–1916. https://doi.org/10.1007/s00531-014-1010-0.
Sunagawa, S., Coelho, L.P., Chaffron, S., Kultima, J.R., Labadie, K., Salazar, G., Djahanschiri, B., Zeller, G., Mende, D.R., Alberti, A., Cornejo-Castillo, F.M., Costea, P.I., Cruaud, C., d'Ovidio, F., Engelen, S., Ferrera, I., Gasol, J.M., Guidi, L., Hildebrand, F., Kokoszka, F., Lepoivre, C., Lima-Mendez, G., Poulain, J., Poulos, B. T., Royo-Llonch, M., Sarmento, H., Vieira-Silva, S., Dimier, C., Picheral, M., Searson, S., Kandels-Lewis, S., Tara Oceans, c., Bowler, C., de Vargas, C., Gorsky, G., Grimsley, N., Hingamp, P., Iudicone, D., Jaillon, O., Not, F., Ogata, H., Pesant, S., Speich, S., Stemmann, L., Sullivan, M.B., Weissenbach, J., Wincker, P., Karsenti, E., Raes, J., Acinas, S.G., Bork, P., 2015. Ocean plankton. Structure and function of the global ocean microbiome. Science 348 (6237), 1261359. https://doi.org/10.1126/science.1261359.
Tobias-Hunefeldt, S.P., Wing, S.R., Espinel-Velasco, N., Baltar, F., Morales, S.E., 2019. Depth and location influence prokaryotic and eukaryotic microbial community structure in New Zealand fjords. Sci. Total Environ. 693, 133507 https://doi.org/10.1016/j.scitotenv.2019.07.313.
Unger, V., Liebner, S., Koebsch, F., Yang, S., Horn, F., Sachs, T., Kallmeyer, J., Knorr, K.-H., Rehder, G., Gottschalk, P., Jurasinski, G., 2021. Congruent changes in microbial community dynamics and ecosystem methane fluxes following natural drought in two restored fens. Soil Biol. Biochem. 160 https://doi.org/10.1016/j.soilbio.2021.108348.
van Vliet, von Meijenfeldt, Dutilh, B.E., Villanueva, L., Sinninghe Damste, Stams, A.J.M., Sanchez-Andrea, I., 2021. The bacterial sulfur cycle in expanding dysoxic and euxinic marine waters. Environ. Microbiol. 23 (6), 2834–2857. https://doi.org/10.1111/1462-2920.15265.
Vigneron, A., Cruaud, P., Pignet, P., Caprais, J.C., Gayet, N., Cambon-Bonavita, M.A., Godfroy, A., Toffin, L., 2014. Bacterial communities and syntrophic associations involved in anaerobic oxidation of methane process of the Sonora Margin cold seeps, Guaymas Basin. Environ. Microbiol. 16 (9), 2777–2790. https://doi.org/10.1111/1462-2920.12324.
Wang, J., Zhang, T., Li, L., Li, J., Feng, Y., Lu, Q., 2017a. The patterns and drivers of bacterial and fungal beta-diversity in a typical dryland ecosystem of northwest China. Front. Microbiol. 8, 2126. https://doi.org/10.3389/fmicb.2017.02126.
Wang, X., Liu, B., Qian, J., Zhang, X., Guo, Y., Su, P., Liang, J., Jin, J., Luan, Z., Chen, D., 2017b. Geophysical evidence for gas hydrate accumulation related to methane seepage in the Taixinan Basin, South China Sea. J. Asian Earth Sci. 168 (DEC), 27–37.
Wei, J., Li, J., Wu, T., Zhang, W., Li, J., Wang, J., Tao, J., Chen, Z., Wu, Z., Chen, W., 2020. Geologically controlled intermittent gas eruption and its impact on bottom water temperature and chemosynthetic communities—a case study in the "HaiMa" cold seeps, South China Sea. Geol. J. 55 (9), 6066–6078. https://doi.org/10.1002/gj.3780.
Wright, J.J., Konwar, K.M., Hallam, S.J., 2012. Microbial ecology of expanding oxygen minimum zones. Nat. Rev. Microbiol. 10 (6), 381–394. https://doi.org/10.1038/nrmicro2778.
Wu, K., Zhao, W., Li, M., Picazo, F., Soininen, J., Shen, J., Zhu, L., Cheng, X., Wang, J., 2020. Taxonomic dependency of beta diversity components in benthic communities of bacteria, diatoms and chironomids along a water-depth gradient. Sci. Total Environ. 741, 140462 https://doi.org/10.1016/j.scitotenv.2020.140462.
Wu, W.X., Logares, R., Huang, B.Q., Hsieh, C.H., 2017. Abundant and rare picoeukaryotic sub-communities present contrasting patterns in the epipelagic waters of marginal seas in the northwestern Pacific Ocean. Environ. Microbiol. 19 (1), 287–300. https://doi.org/10.1111/1462-2920.13606.
Xia, X., Guo, W., Liu, H., 2017. Basin scale variation on the composition and diversity of archaea in the Pacific Ocean. Front. Microbiol. 8, 2057. https://doi.org/10.3389/fmicb.2017.02057.
Xue, Y., Chen, H., Yang, J.R., Liu, M., Huang, B., Yang, J., 2018. Distinct patterns and processes of abundant and rare eukaryotic plankton communities following a reservoir cyanobacterial bloom. ISME J. 12 (9), 2263–2277. https://doi.org/10.1038/s41396-018-0159-0.
Zhang, Y., Qin, W., Hou, L., Zakem, E.J., Wan, X., Zhao, Z., Liu, L., Hunt, K.A., Jiao, N., Kao, S.J., Tang, K., Xie, X., Shen, J., Li, Y., Chen, M., Dai, X., Liu, C., Deng, W., Dai, M., Ingalls, A.E., Stahl, D.A., Herndl, G.J., 2020d. Nitrifier adaptation to low energy flux controls inventory of reduced nitrogen in the dark ocean. Proc. Natl. Acad. Sci. U. S. A. 117 (9), 4823–4830. https://doi.org/10.1073/pnas.1912367117.
Zhang, T., Xu, S., Yan, R., Wang, R., Gao, Y., Kong, M., Yi, Q., Zhang, Y., 2022. Similar geographic patterns but distinct assembly processes of abundant and rare bacterioplankton communities in river networks of the Taihu Basin. Water Res. 211, 118057 https://doi.org/10.1016/j.watres.2022.118057.
Zhang, Y., Jing, H., Peng, X., 2020c. Vertical shifts of particle-attached and free-living prokaryotes in the water column above the cold seeps of the South China Sea. Mar. Pollut. Bull. 156, 111230 https://doi.org/10.1016/j.marpolbul.2020.111230.

Zhang, X., Liu, S., Wang, J., Huang, Y., Freedman, Z., Fu, S., Liu, K., Wang, H., Li, X., Yao, M., Liu, X., Schuler, J., 2020b. Local community assembly mechanisms shape soil bacterial beta diversity patterns along a latitudinal gradient. Nat. Commun. 11 (1), 5428. https://doi.org/10.1038/s41467-020-19228-4.

Zhang, W., Pan, Y., Yang, J., Chen, H., Holohan, B., Vaudrey, J., Lin, S., McManus, G.B., 2018. The diversity and biogeography of abundant and rare intertidal marine microeukaryotes explained by environment and dispersal limitation. Environ. Microbiol. 20 (2), 462–476. https://doi.org/10.1111/1462-2920.13916.

Zhang, H., Hou, F., Xie, W., Wang, K., Zhou, X., Zhang, D., Zhu, X., 2020a. Interaction and assembly processes of abundant and rare microbial communities during a diatom bloom process. Environ. Microbiol. 22 (5), 1707–1719. https://doi.org/10.1111/1462-2920.14820.

Zhang, Y., Yao, P., Sun, C., Li, S., Shi, X., Zhang, X.H., Liu, J., 2021. Vertical diversity and association pattern of total, abundant and rare microbial communities in deep-sea sediments. Mol. Ecol. 30 (12), 2800–2816. https://doi.org/10.1111/mec.15937.